NAIST-IS-DD1361015

Doctoral Dissertation

Human-Safe and Robot-Efficient Control for Close-Proximity Human-Robot Interaction

Gustavo Alfonso GARCIA RICARDEZ

March 14, 2016

Graduate School of Information Science
Nara Institute of Science and Technology

A Doctoral Dissertation
submitted to the Graduate School of Information Science,
Nara Institute of Science and Technology
in partial fulfillment of the requirements for the degree of
Doctor of ENGINEERING

Gustavo Alfonso GARCIA RICARDEZ

Thesis Committee:

Professor Tsukasa Ogasawara	(Supervisor)
Professor Norihiro Hagita	(Co-supervisor)
Associate Professor Jun Takamatsu	(Co-supervisor)
Postdoctoral Fellow Akihiko Yamaguchi	(Carnegie Mellon University)

Human-Safe and Robot-Efficient Control for Close-Proximity Human-Robot Interaction*

Gustavo Alfonso GARCIA RICARDEZ

Abstract

With the increasing physical proximity of Human-Robot Interaction (HRI), ensuring that robots do not harm surrounding humans has become crucial. This requires new methodologies to endow robots with the ability to keep human safety when operating in close proximity of humans.

This dissertation proposes heuristic and analytical solutions to the open problem of human safety. The heuristic solutions are based on the human notion of danger while the analytical solutions are supported by physical measurements. With a focus on the pre-collision stage of HRI, the proposed solutions decrease the risk of a collision and the potential human injuries if a collision occurs. While this dissertation prioritizes human safety, it also targets to maintain the robot's efficiency.

In the heuristic approach, this dissertation proposes *Asymmetric Velocity Moderation* (AVM) as a low-level controller for robotic systems to enforce human-safe motions. To avoid collisions, AVM considers the distance of multiple points on the human and on the robot, as well as the direction of the motion. AVM solves the trade-off between safety and efficiency with an asymmetric speed restriction: stricter when moving toward the human and less strict when moving away from the human. A *Withdrawal* strategy which increases the distance between the human and the robot when they are too close is proposed. This strategy resembles to some extent the reflexive reaction of a human withdrawing his arm when another human is simultaneously trying to reach the same region.

*Doctoral Dissertation, Graduate School of Information Science, Nara Institute of Science and Technology, NAIST-IS-DD1361015, March 14, 2016.

In the analytical approach, a human safety metric based on human behavior estimation and impact severity is developed. This *Safety Index* (SI) estimates the most dangerous situation for the human and how severe the injuries inflicted to the human would be if a collision occurs in that situation. A flexible controller *Generalized Velocity Moderation* (GVM) capable of using different human safety metrics in an interchangeable manner is also developed. This controller keeps the human safety by modifying the robot speed to comply with a safety constraint while minimizing the impact on the robot's efficiency.

Through real-robot and simulation experiments using the human-size humanoid robot HRP-4 in HRI scenarios and dangerous situations, this dissertation demonstrates that the proposed methods are able to keep human safety with a competitive robot's performance.

Keywords:

human safety, safety index, robot control, human-robot interaction, humanoid

ヒューマン・ロボット・インタラクションのための安全かつ効率的な制御手法に関する研究*

Gustavo Alfonso GARCIA RICARDEZ

内容梗概

ロボット分野の研究が進むにつれて，人間とロボットのインタラクションにおいて物理的な近接の機会が増えていることから，ロボットが周囲の人間に危害を加えないことを保証することは重要な課題となる．ロボットが人間の近くで動作する際に，ロボットに人間との安全性を考慮させる技術が必要となる．本論文では，人間とロボットとの安全性といった未解決問題に対してヒューリスティックと解析的な解法を提案する．

ヒューリスティックを用いた解法は人間の危険の概念に基づいており，解析的な解法は物理的な測定に基づいてた提案をされている．ヒューマン・ロボット・インタラクション (HRI) の中の衝突前の状況で，提案手法は人間にぶつかるリスクと潜在的な人間への傷害を減らすことができる．人間への安全を考慮することは重要であるが，提案手法では安全性とロボットの動作効率の両立を目的としている．ヒューリスティックな解法のために，人間に対して安全な動作を実施するロボットシステムのコントローラとして，Asymmetric Velocity Moderation (AVM) を提案する．人間との衝突を回避するために，AVM はロボットと人間との複数点間の距離と両者の動作の方向を考慮する．AVM は，非対称速度制限を用いることで安全性と効率を両立を解決する．非対称速度制限は，人間に向かって動作する場合に速度を制限し，人間から離れる場合には速度を制約しない手法である．ロボットが人間に極めて近い場合に，ロボットを人間から離す方法として Withdrawal を提案する．Withdrawal は，人間と人間が同じ領域に同時に近付こうとしているときに腕を引き抜くような反射的な反応の動作を，ロボットに適用する方法である．

*奈良先端科学技術大学院大学 情報科学研究科 博士論文, NAIST-IS-DD1361015, 2016 年 3 月 14 日.

解析的な方法では，人間の行動の推定と衝突の程度に基いた，ロボットにおける人間との安全性の定量化する方法を開発する．安全の指標は，最も危険な状況や，人間に対して衝突が起こりうる状況で障害がどの程度ひどいかを推定する．GVM は，ロボットの動作効率に対しての影響を最小限に抑える一方で，人間との安全のための制約に適合するようにロボットの速度を調整すること．

HRI や危険な状況において，人間サイズのヒューマノイドロボット HRP-4 を用いた実機と動力学シミュレータを用いた実験を通じて，提案手法が高効率を保ち人間の安全性を保証できることを示す．

キーワード

人間の安全性, 安全性の指数, ロボット制御, ヒューマン・ロボット・インタラクション, 人間型ロボット

Acknowledgements

The enterprise of obtaining a Ph.D. degree leaves in this dissertation the testimony of a challenging road whose obstacles I would not have overcome alone.

First, I wish to express my most sincere gratitude to Professor Tsukasa Ogasawara for accepting me as a student in his laboratory and for supporting me to complete this endeavor. His kindness and wisdom has been always the emblem of his guidance. I will always thank him for making this dream come true.

I am very grateful to Associate Professor Jun Takamatsu for sharing his immense knowledge and his passion for Robotics. His always insightful comments and questions guided me to a widened world of possibilities.

I would like to express my deepest thanks to Dr. Akihiko Yamaguchi, my adviser, for his nurturing guidance and his encouragement to face all challenges. His generous advice and his patience allowed me to fulfill this quest.

I am also grateful to Dr. Atsutoshi Ikeda for his friendliness and his valuable comments which always were a great motivation.

I wish to deeply thank my thesis committee: Professor Tsukasa Ogasawara, Professor Norihiro Hagita, Associate Professor Jun Takamatsu, and Postdoctoral Fellow Akihiko Yamaguchi for their helpful comments and their constructive criticism.

I am profoundly grateful to the Japanese Government for granting me the MEXT Scholarship. Their generosity made my dream of studying in Japan come true.

I would like to thank from the bottom of my heart to my loving family for their incommensurable affection and understanding. Specially to my mother who

has always encouraged me to accomplish my goals. Her infinite love makes me feel I am always close home. To my grandmother for filling my days of happiness with our transpacific conversations. To my sister for making me see the things the way they truly are and for the two pieces of heaven she brought to my life: my niece Alaia and my nephew Dominick.

To Lulu and Fernando for their love and for being always there for me. Our dominical video conferences and the constant advice of my dear *tomodachi* have always revitalized my drained energies and have been a great shield against frustration.

To the Nara Institute of Science and Technology for opening its doors to me and for making my stay as international student a very pleasant experience. Thanks to all the students and staff for your kindness and help.

I would like to thank all my friends who at some point shared with me this amazing journey. As it is impossible to mention them all, it is also impossible to forget the great moments we spent together. I owe special thanks to Abdulraheem Shaqiqat who became my brother in Japan and for life. To my dearest friends Lis Kanashiro, Doudou Fall, Diego Reinoso, and Nelson Kibinge whose support and friendship during these years made this odyssey possible.

Last but not least, to the Robotics Lab for giving me the wonderful opportunity of doing my research. Specially, I would like to thank my dearest friend Satoki Tsuichihara who has been a true accomplice in this adventure. His always available help and his unlimited kindness made my life in Robotics Lab great. To all my labmates for helping me with everything, from my Japanese language to my life in Japan and my experiments.

Contents

List of Figures

A humble brick to build the First Law of Robotics.

A robot may not injure a human being, or, through inaction, allow a human being to come to harm.
Isaac Asimov
("I, Robot," 1950.)

Chapter 1

Introduction

As robotic technologies advance, the potential applications of robots are increasing. The robot-in-a-cage paradigm has pushed industrial development in the last decades. In recent years, that paradigm has come to a crossroad risen by the necessity of robotic applications in daily life environments. To venture in human populated environments, the fence-free robots need a new ability that their classic industrial counterparts do not: keeping the surrounding humans unharmed.

This dissertation proposes new methodologies to endow robots with the ability of keeping humans safe during the interaction. These methodologies are oriented to robots that interact with humans in a daily basis, such as service robots. The proposed methods were tested using real-robot experiments as well as simulation, analyzing the safety features and reporting the robot's efficiency.

1.1. Motivation and objective

Human safety is a crucial issue for the coexisting of humans and robots in our daily life environment. Skillful robots are well on the way toward a coming era of robots in every home [1]. Ogorodnikova discusses the potential economical and social benefits of the symbiosis between humans and robots which are driving this transition [2]. However, to cross this horizon, robots must be able to operate around humans without endangering them and to complete their tasks efficiently.

Solving human safety issues while also considering the robot's efficiency plays

an important role in the integration of humans' and robot's workspaces [3, 4, 5, 6, 7]. This is because we need fast and powerful robots to perform a variety of tasks, ranging from the repetitive and tedious to the life-critical, in environments populated by humans such as houses, offices, hospitals, factories, or even in rescue scenarios. We need robots to do such tasks in a flawless Human-Robot Interaction (HRI) where humans and robots share their workspaces.

The focus of this dissertation lies on solving human safety challenges when human and robot are interacting in close proximity. It is at this short separation where the human is within the kinematic reachability of the robot. Even though the physical integrity of the human is at risk in this vicinity, it is also at this distance where we require robots to perform tasks in our environments. Robot tasks such as washing dishes in a kitchen, sorting packages in an office, picking groceries in a supermarket, clearing tables in a restaurant, solving puzzles with children in a school, they all have in common the eventual irruption of humans in the robot workspace. When such irruptions occur, the HRI is closer and the risk of injuring humans rises. At such increased level of HRI, new methodologies that enable robots to be both safe and efficiency when moving in human proximity are required.

In this dissertation, human safety is about controlling the risk of a collision with the human, as well as reducing the potential injuries as a consequence of a collision. The perspective of human safety presented in this work is based on a physical point of view, as opposed to a psychological point of view where aspects such as the sense of safety and comfort are considered.

The priority of the human safety in this work is to avoid collisions. If a collision occurs, that collision should occur while the robot is completely stopped. Secondly, reducing the speed of the robot is assumed to make the interaction safer for the human. Thirdly, unnecessary human proximity should be avoided.

This dissertation proposes solutions to human safety challenges of HRI in close proximity which are characterized by: a) a limited time for the robot to react to the human motions; b) a latent risk of a collision due to erratic human motions; c) the risk of inflicting injuries to the human if a collision occurs; and d) the potential obstruction of the human target by the robot. As this dissertation focuses on the pre-collision phase of HRI, approaches such as compliant control

[8] escape from the scope of this work.

Previous methods proposed by Sisbot *et al.* [9, 10] consider distance, while the method proposed by Tsai *et al.* [11] considers the distance and momentum of the robot links. Kulic *et al.* consider the distance between centers of mass and provide a robot restriction with a bivalent direction of motion (i.e., away and toward) [12]. The solutions proposed in this dissertation further the applicable robot restrictions to virtually any direction. We use distance and the angle between the displacement vector and the velocity vector to derive the robot restrictions. Then we apply this idea to the human and robot's bodies to consider the whole-body relationship.

In a previous work of Ikuta *et al.*, human safety is estimated based on the impact force [13]. Human safety is evaluated from the ratio between that impact force and the minimum force necessary to injure humans. The novelty of the safety index proposed in this dissertation lies on modeling the human behavior so that it maximizes the potential injuries of a collision. Then, the seriousness of a collision between an estimated human state and a future robot state is determined through physical models and used to evaluate the human safety.. In other words, the proposal of this dissertation makes the robot anticipate the worst scenario and be able to avoid potential injuries to keep the human safe.

1.2. Contributions

The contributions of this research are fourfold. First, a controller to keep the human safety with an embedded human safety metric based on distance and direction of motion. Second, a reflexive response to increase the distance to human when the human and robot get too close. Third, a human safety metric based on the severity of potential human injuries and human behavior estimation. Forth, a controller to keep human safety that can use multiple human safety metrics. The following is a brief description of each contribution:

1. An easily-implementable and widely-applicable robot controller for human safety. This reactive controller considers the whole-body relationship between the human and the robot, using distance and the direction of the motion. The controller keeps human safety by reducing the speed of the

robot in an asymmetric way. This asymmetric property benefits the robot's efficiency without compromising human safety. (*Asymmetric Velocity Moderation* or *AVM*, Section 3.1).

2. A behavior-specific strategy that increases the distance to human when human and robot are too close. This strategy aims to temporarily increase the distance to the human since it is natural to consider that the possibility of a collision decreases as distance increases. Withdrawal strategy resembles to some extent the motion that a human does when trying to reach a region that another human is simultaneously trying to reach and withdraws his arm. (*Withdrawal*, Section 3.2)

3. A human safety metric based on human behavior estimation and the potential damage of a collision between human and robot. This new method to assess human safety calculates the impact severity of a collision which may occur if the human does the most dangerous motion. This method is a solution to the human safety challenge which anticipates the human motion. (*Safety Index* or *SI*, Section 4.1).

4. A flexible controller for human safety capable of using different human safety metrics in an interchangeable manner. This opens the possibility to use other researchers' safety metrics or new human safety standards as soon as they are released. This controller keeps the human safety by reducing the speed of the robot to comply with a safety constraint. Also, this controllers uses the maximum speed that complies with the safety constraint to maintain the robot's efficiency. (*Generalized Velocity Moderation* or *GVM*, Section 4.2).

1.3. Approach

Human safety as the absolute lack of collisions between the humans and the robots is idealistic. This is because of the dynamic nature of the interaction with erratically and constantly moving humans. In realistic terms, human safety is about controlling the risk of a collision to levels that allow the coexistence of humans and robots.

Furthermore, as the risk of a collision remains latent, the robot should maintain the harshness of the potential injuries to human, derived from the collision, to acceptable levels in terms of the nature of the application.

The target scenarios of this dissertation are daily life environments such as houses, offices, and hospitals where the robot performs manipulation tasks such as washing dishes in a kitchen, sorting packages in an office, picking groceries in a supermarket, clearing tables in a restaurant, solving puzzles with children in a school. As the robot executes the task, humans are expected to irrupt. The robot should be able to cope with these irruptions, guaranteeing the human safety and keeping a its performance.

The focus of this dissertation is on human safety when human and robot are in close proximity. At close proximity, the interaction between human and robot is expected to take place considering the target scenarios. It is also at this distance where the probability of a collision is higher as the human is within the robot's kinematic reachability. Therefore, the robot motion should be quickly modified to decrease the probability of a collision.

This dissertation adopts the physical point of view of human safety, as opposed to the psychological point of view where aspects such as sense of safety and comfort are treated. By considering the physical aspects of human safety, this dissertation attempts to eliminate vices of HRI such as: the familiarity to dangerous situations brought by the repetition of safety-ill interactions; the potential danger misjudgment by kids, elder people, or people with different abilities; and the tendency to attribute super-human to robots where users may mistakenly think that robots cannot harm them.

1.4. Overview of proposed methods

First, human safety is approached in a heuristic way. Factors as the distance and the direction of motion dictate the modifications to the robot behavior. These factors were chosen as an intuitive notion of safety. The robot reacts to the human motion by reducing the speed or increasing the distance, which can be considered *natural* reactions. As this approach follows the human notion of danger rather than physical measurements, some situations that can be physically proved to be

dangerous may be overlooked by the heuristic approach.

The analytical approach to human safety proposed in this dissertation is based on physical models. The danger is calculated from the potential injuries of a collision. Moreover, the human behavior is modeled to maximize this danger. With the human motion prediction and the knowledge of potential injuries, the robot can avoid situations whose danger exceeds an acceptable level.

Following the heuristic approach, we propose the Asymmetric Velocity Moderation controller to restrict the robot motion until is safe for the human. Also, we propose the Withdrawal strategy as a reflexive response to situations where human and robot are too close. Following the analytical approach, the Safety Index which scores the human safety given a situation and a robot control input. Moreover, we develop the Generalized Velocity Moderation controller to make the robot comply with a safety constraint. The overview of each method is as follows:

Asymmetric Velocity Moderation (AVM)

AVM is a solution to the human safety problem which consists of a controller with an embedded safety metric. AVM restricts the robot speed according to the distance and the direction of the motion. While this method prioritizes human safety, it also keeps a competitive robot performance. AVM considers multiple points on the human and on the robot to restrict the robot speed. The key idea of AVM is to restrict the robot speed in an asymmetric way: a strict restriction for motions toward the human and a relaxed restriction for motions away from the human.

Withdrawal

Withdrawal strategy increases the distance between the human and the robot when they are too close. This is because the probability of a collision is decreases with a greater distance. Withdrawal uses a virtual force model defined by a repelling force exerted by the human and an attractive force exerted by a parking position. The resulting virtual force drives the end-effector away from the human and toward the parking position. After the deviation from the original trajectory

caused by the proximity with the human, Withdrawal returns to the configuration where it was engaged to continue with the task.

Safety Index (SI)

SI solves the problem of the prediction of human motion and the connection to the potential human injuries. SI is human safety metric based on the impact severity of a collision between human and robot. SI estimates the most dangerous human motion, i.e., the one that maximizes the impact severity. The collision where the impact severity is calculated does not actually happen. This is because this collision is assumed to occur between an estimated human state and a future robot state.

Generalized Velocity Moderation (GVM)

GVM is a flexible controller capable of using human safety metrics in an interchangeable way. The purpose of GVM is to move the robot as fast as possible while satisfying a safety constraint. The safety constraint is based on the human safety metric used and it dictates the trade-off between human safety and efficiency.

The methods proposed in this dissertation are intended to be widely applicable but they are more suitable for service and industrial robotic applications. Numerous tasks in these applications (e.g., pick-and-place) usually require a collision-free interaction. The proposed control and evaluation methods are designed for the human safety during the pre-collision phase of the interaction. In other fields such as health care or rescue robotics, the methods proposed here are partially applicable as contact (i.e., a controlled collision) is usually required, which is out of the scope of this dissertation.

1.5. Dissertation layout

The rest of this dissertation is organized as follows:

Chapter 2 This chapter introduces the idea of robot control for human safety. First, it provides a general overview of the human safety challenges. Then, a review of the related work is presented.

Chapter 3 This chapter proposes a heuristic approach to robot control for human safety. First, the Asymmetric Velocity Moderation (AVM) controller is detailed. Second, the Withdrawal strategy is presented. Also, the experimental setup, the test cases and HRI scenarios are introduced. Finally, the experimental results both with a real robot and in simulation are discussed.

Chapter 4 This chapter proposes an analytical approach to robot control for human safety. First, a new human safety metric based on human behavior estimation and impact severity is detailed. Second, a Generalized Velocity Moderation (GVM) controller capable of using various safety metrics is presented. The final section of this chapter includes the experimental results.

Chapter 5 This final chapter concludes the dissertation and highlights the features of the proposed methods. Additionally, some possible directions of future work are presented.

Summary

- The motivation of this dissertation is the necessity of keeping the humans unharmed when interacting with robots in close proximity.
- Our objective is to develop robot behaviors that enable human-safe interactions.
- The contributions of this dissertation are four methods: AVM (controller and human safety metric), Withdrawal (reflexive response for collision avoidance), SI (human safety metric), and GVM (controller for multiple human safety metrics).
- We solve the human safety problem by following two approaches: heuristic and analytical.
- The heuristic approach is based on the human notion of danger while the analytical approach is based on physical models.

Chapter 2

Human safety in Human-Robot Interaction

Under their role of task-burden relievers, robots have found transcendent applications in daily-life environments, such as houses, offices, and hospitals. In these scenarios, the pragmatic solution of isolating humans and robots can easily reach the point of obsolescence. Therefore, robots have been released from conventional confinements and brought into the human populated world. Nevertheless, these fence-free robots must posses a very particular ability: human safety. As explained by Fraichard, the human safety problem remains open in spite of substantial efforts toward a human-safe interaction [14].

This chapter reviews the existing work on human safety. Previous work in the field of human safety includes safety standards, several approaches to the interaction of humans and robots, and efforts to evaluate safety.

2.1. Standardization

This section summarizes the most relevant standards to human safety as studied in this dissertation, as well as the initiatives from robotics companies.

2.1.1 ISO

An initial step to norm human safety during human-robot interaction is found in the ISO 10218, where a safe robot speed is established [15]. Also, this standard requires robots to cause mild injuries, if any.

The ISO 13482 describes a safety-related speed control, however it is mainly applicable to mobile robots and exoskeletons [16]. This dissertation investigates the further challenge of human interaction with more complicated robots such as humanoid robots.

The technical specification TS 15066 is an ongoing effort to delineate the safety requirements of collaborative operations [17]. Nevertheless, this specification has not been published at the time of this dissertation, which leaves the previously mentioned standards as the primary guidelines.

2.1.2 Other initiatives

Recently, robotics companies such as ABB[1] and Robotiq[2] are documenting their experience and proposals about human safety. These initiatives create awareness of the human safety problem and push towards the standardization of human safety.

2.2. Collision phases

We can divide the existing work by looking at the collision event into two phases: pre-collision and post-collision. Methods for collision avoidance are oriented to the pre-collision phase while methods coping with the collision itself are oriented to the post-collision phase.

2.2.1 Pre-collision

A reactive strategy driven by a safety index is proposed by Kulic *et al.* [18]. Such safety index considers the inertia and the distance between the centers of

[1]ABB Safety Systems, http://new.abb.com/control-systems/safety-systems
[2]Robotiq Ebooks, http://robotiq.com/resource-center/ebooks/

mass of the human and robot. This work inspired the controllers proposed in this dissertation. However, we use multiple distances distributed along both human and robot bodies to calculate a specific restriction for every direction of the robot motion. This benefits the robot's efficiency without undermining human safety because with the proposed scheme the robot can move away from the human even if they are very close.

Safety planners such as the human-aware manipulation planner proposed by Sisbot *et al.* use safety, human visibility and comfort as cost functions for planning [9, 19, 10]. The authors assess human safety considering only the distance to the human. We also consider the direction of the motion which enables to know if the robot moves toward or away from the human.

The work of Ding *et al.* estimates the human arm motion to generate a forbidden region that the planner should avoid [20]. The present dissertation estimates the human behavior by considering the position of multiple points on the human to evaluate human safety.

2.2.2 Post-collision

The research of Heinzmann *et al.* proposes to restrict the torque to comply with a safety restriction [21]. The safety restriction limits the potential impact force of a collision. This dissertation also analyzes the forces at impact but in the ambit of a collision which occurs with an estimated human state obtained from the most dangerous motion the human could do.

The work of Haddadin *et al.* made the robot compliant to external forces [8]. The safety of the interaction is based on reducing the impact severity when a collision occurs. Parusel *et al.* propose a control architecture to generate different behaviors mainly focusing in a collision-based interaction with humans [22]. This dissertation modifies the robot's motion before the collision, while compliance is used during the collision.

The design of robot surfaces to minimize the stress of collisions has been studied by Park *et al.* [23].

2.3. Objective evaluation of human safety

The safety indexes reviewed in this work are classified in distance-related and injury-related. Another criteria to classify safety indexes in distance-based and force-based is proposed by Ogorodnikova [24].

2.3.1 Distance-related

The method proposed by Kotosaka *et al.* evaluates the frequency of exposure to harm based on the average minimum distance during the task execution, and based on the distribution of the maximum velocity [25].

Lacevic *et al.* propose another safety evaluation method called *kinetostatic danger field* (KSDF) which considers the direction of the robot's motion [26, 27]. The authors exploit kinematic redundancy to obtain safer postures. The KSDF estimates the danger of the whole kinematic chain as the superposition of the danger generated by its links. In contrast, this dissertation uses independent measurements of the danger generated by every point on the robot to avoid overrestricting the robot speed and negatively impacting the overall performance.

Tsai *et al.* evaluated safety using distance and the robot link momentum [11]. The authors use ellipsoids around the robot links to simplify the distance calculation. Nevertheless, dangerous points on the robot link which are critical for safety assessment may be neglected in the simplification of Tsai *et al.*, while these points can be explicitly selected as representative points in the scheme proposed in this dissertation.

2.3.2 Injury-related

Haddadin *et al.* estimate safety using injury evaluation through crash-testing [28, 29], while Ogure *et al.* proposed to use hazard analysis [30]. This dissertation approaches safety differently. The first focus is on robot control so a simple but reliable safety index based on the target robot velocity and its relationship with the whole human body is used. Then, a human safety metric is developed based on the potential injuries that the robot can inflict to the human and using human behavior estimation to anticipate the human most dangerous motion.

The relation between inertia, velocity, and geometry at possible impact locations to the resulting injury of a collision is studied by Haddadin *et al.* [31]. Then, the obtained knowledge about injuries is used for control. A safety index based on head injury indexes from the automobile industry is proposed by Echavarri *et al.* [32].

Ikuta *et al.* proposed a safety index based on impact force and impact stress [13]. The proposed human safety metric was inspired by such work where safety is evaluated as the ratio between an impact force and a critical impact force. The critical impact force is the minimum impact force required to injure humans. In this dissertation, the danger is associated to the injuries a robot can inflict to a human if a collision occurs. The harshness of the injuries derives from the impact severity of the collision.

Summary

- Current human safety standards are general and have a limited applicability to HRI in close proximity.
- This dissertation investigates the further challenge of human interaction with more complicated robots such as humanoid robots.
- Related works on human safety focus on the pre-collision phase and on the post-collision phase of HRI.
- Focusing on the pre-collision phase, this dissertation proposes methods to reduce the risk of a collision.
- This dissertation also proposes methods to objectively evaluate human safety based on distance, motion direction, and injuries.

Chapter 3

Heuristic approach

This chapter describes a heuristic approach to robot control for human safety. The proposed AVM assesses human safety using the distance and the direction of the motion, which solves human safety in an intuitive manner. The purpose of AVM is to achieve a simple but reliable method to produce a human-safe robot behavior. Moreover, this chapter introduces the Withdrawal strategy which mimics, at some extent, the arm withdrawal motion of two humans simultaneously attempting to reach the same space but increasing the distance as a reflex to avoid collision.

Real-robot and simulation experiments where the human and robot perform simple tasks while they share their workspaces are performed. The experimental results validate the use of AVM as a low-level controller for human safety that benefits both human safety and the robot's performance. Moreover, experiments are carried out with Withdrawal strategy as a higher-level controller whose motion is audited by AVM to guarantee human safety.

This chapter is organized as follows. Section 3.1 details the proposed AVM controller and its embedded safety index. Section 3.2 presents the Withdrawal strategy. Section 3.3 introduces the experimental setup. Finally, Section 3.4 reports the experimental results.

3.1. Asymmetric Velocity Moderation

This section proposes Asymmetric Velocity Moderation (AVM) as a low-level controller to keep human safety. To ensure human safety, we consider the relationship between the whole body of both human and robot. According to the relationship of their whole bodies, we restrict the robot speed because we assume that the lower the speed, the safer the robot motion is. The idea behind AVM is to restrict the speed of the robot when the robot is moving toward the human but relax this restriction when the robot is moving away from the human. Thus, AVM maintains task performance as much as possible without sacrificing human safety.

The proposed AVM is directly applicable to tasks whose velocity is not essential, such as pick-and-place. For tasks that depend on specific velocities, such as catching a ball, a higher-level planner is necessary.

The rest of this section is organized as follows. Section 3.1.1 provides an overview of AVM. Section 3.1.3 describes the details of the proposed algorithm. Section 3.1.2 explains how the asymmetric property of AVM is achieved.

3.1.1 Overview

AVM is a low-level controller intended to ensure human safety while maintaining the efficiency of a robot's performance in accomplishing a task. Keeping the human safety is achieved by restricting the speed of the robot. The core idea of AVM to consider both human safety and the robot's performance is an asymmetric velocity restriction, which depends on the direction of the robot's movement.

The input of AVM is a trajectory of joint angles. The output of AVM is the target joint angles to follow the trajectory in an on-line manner, where speed is restricted to ensure the human safety. The speed is restricted by temporarily remapping the points on the trajectory without modifying the original shape of the motion.[3] This does not affect the task completeness, under the assumption that the task is described by the shape of the trajectory rather than its velocities.

AVM considers every combination of representative points on the robot and

[3]This concept is similar to the trajectory scaling presented by Haddadin [7] and Szadeczky-Kardoss *et al.* [33].

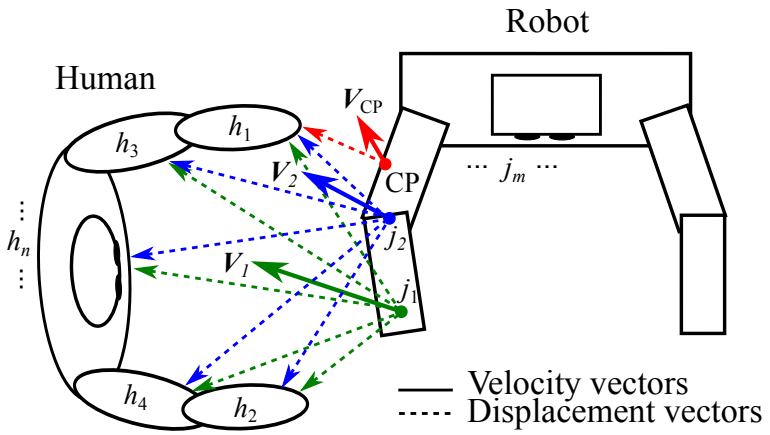

Figure 3.1: AVM considers the whole-body interaction. Points j on the robot and h human links are used by AVM. The continuous arrows depict the velocity vectors while the dotted arrows represent the displacement vectors.

on the human body. First, we calculate a speed restriction for every possible pair of points, one on the robot and one on the human. Then, we choose the most restrictive one for the actual temporal-remapping.

As illustrated in Figure 3.1, AVM considers the whole-body interaction by using multiple points on both the human and the robot. Here, AVM considers all points j on the robot and all human links h. Moreover, AVM uses two points on the robot's joints and the closest point (CP) to determine whether the robot speed needs to be restricted to keep the human safe.

3.1.2 Asymmetric restriction

There are two key ideas used in AVM to compute the speed limitation v_{jh}^{limit}. One is to apply an asymmetric restriction and the other is to consider three distance ranges.

The three ranges are *too close*, *close*, and *far enough*, as shown in Figure 3.2. Two thresholds D_{min} and D_{max} are used to define these ranges. In each range, the method to obtain the speed restriction is different. In the *far enough* range, the robot can move at the allowable maximum speed V_{safe}. In the *close* range, the robot motion is more restricted toward the human and less restricted away from

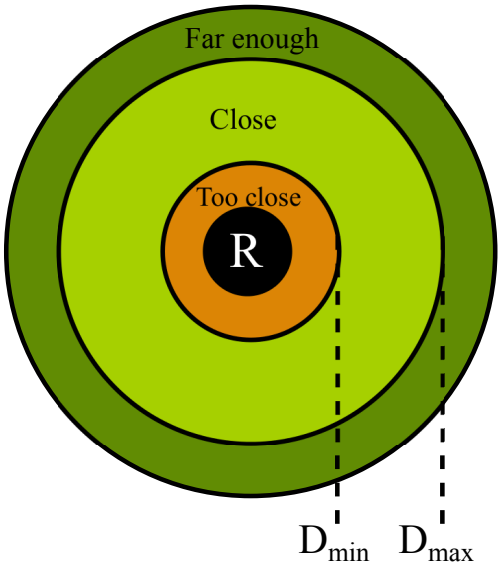

Figure 3.2: Division of distance ranges with the $D_{\min}$ and $D_{\max}$ thresholds.

the human. In the *too close* range, the robot can take only a limited movement, i.e., moving slowly away from the human but not toward the human. To choose $D_{\min}$ and $D_{\max}$, we consider the reactiveness of the system, the sensors' reliability, and V_{safe}.

The asymmetric restriction is created by using the speed limitation v_{jh}^{limit} which is given by the product of $f(d_{jh}, \theta_{jh})$ and V_{safe}, where θ_{jh} is the angle between the displacement and velocity vectors, as depicted in Figure 3.3. The function $f : \mathbb{R} \to [0, 1]$ is defined as follows:

$$f(d_{jh}, \theta_{jh}) = \begin{cases} f^{\text{aux}}(D_{\min}, \theta_{jh}) & (d_{jh} \leq D_{\min}) \\ f^{\text{aux}}(d_{jh}, \theta_{jh}) & (D_{\min} < d_{jh} \leq D_{\max}), \\ 1 & (D_{\max} < d_{jh}) \end{cases} \tag{3.1}$$

where f^{aux} is a function with a limited distance range.

The function f^{aux} is calculated using an auxiliary circle, shown in Figure 3.4. The auxiliary circle has no physical meaning, but it is used to relate the distance and the direction of the motion. Considering the horizontal diameter of the circle, we set one side as the human side, and the opposite side as the robot side. The asymmetricity with respect to θ_{jh} is calculated with the modified center O'; f_{aux}

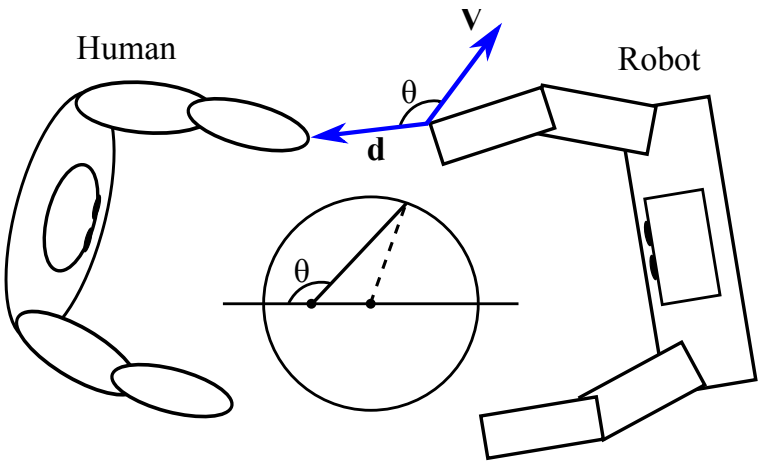

Figure 3.3: Displacement **d** and velocity vectors **V**, and the angle θ that they form are used by AVM to relate the distance and the direction of motion.

corresponds to the length from O' to a point on the circle. The circle expands and shrinks linearly according to the distance d_{jh}, as shown in Figure 3.5. Also, the shifted center O' moves in a linear way according to the distance. When $D_{\max} \leq d_{jh}$, O' coincides with the circle's center O. When $d_{jh} \leq D_{\min}$, O' is at the intersection of the horizontal diameter and the circumference at the left of the circle, i.e., next to the human side. The circle radius and O' are invariant to θ_{jh}. As O' is closer to the human side, the speed restriction increases in the direction of the human.

The function f^{aux} is calculated from r and r' using the Law of Cosines, as follows:

$$f^{\text{aux}}(d_{jh}, \theta_{jh}) = r' \cos(\pi - \theta_{jh}) + \sqrt{r'^2 \cos^2(\pi - \theta_{jh}) + r^2 - r'^2}. \qquad (3.2)$$

where r and r' depend on d_{jh}, i.e., $r(d_{jh})$ and $r'(d_{jh})$.

The function f^{aux} is designed to meet the following requirements. If d_{jh} is $D_{\max}$, f^{aux} takes the value of 1 regardless of θ_{jh}, where $r(d_{jh}) = 1$, $r'(d_{jh}) = 0$. If d_{jh} is $D_{\min}$, f^{aux} takes the value of 0 for $\theta_{jh} = 0$ (i.e., moving toward the human), and f^{aux} takes the value of F_{rec} for $\theta_{jh} = \pi$ (i.e., moving away from the human); here, $r(d_{jh}) = r'(d_{jh}) = \frac{F_{\text{rec}}}{2}$. The circle's radius r and the length r' are linear to the distance d_{jh}. The equations of r and r' that fulfill these requirements are as

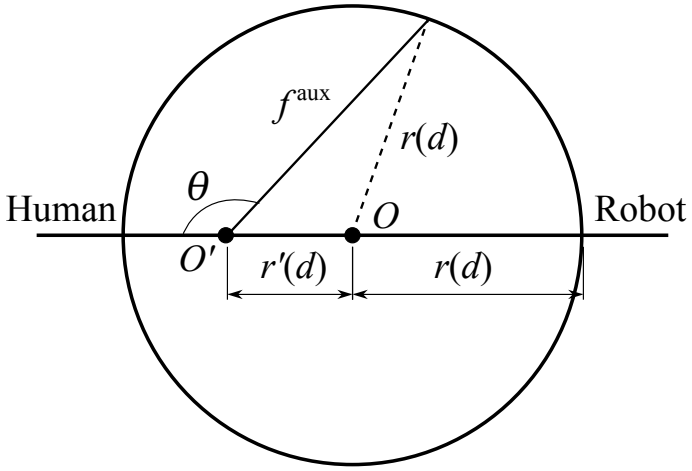

Figure 3.4: The proposed auxiliary circle to calculate f^{aux}.

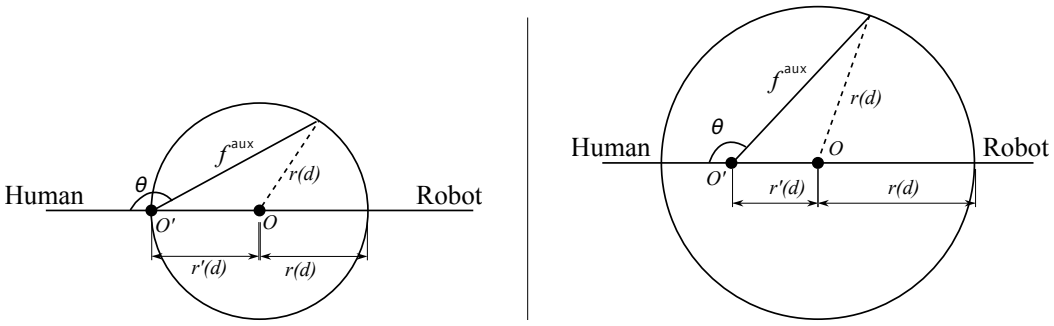

(a) $||\mathbf{d}|| \leq D_{\min}$ (b) $D_{\min} < \|\mathbf{d}\| < D_{\max}$

Figure 3.5: Circle shrinks and expands according to $||\mathbf{d}||$.

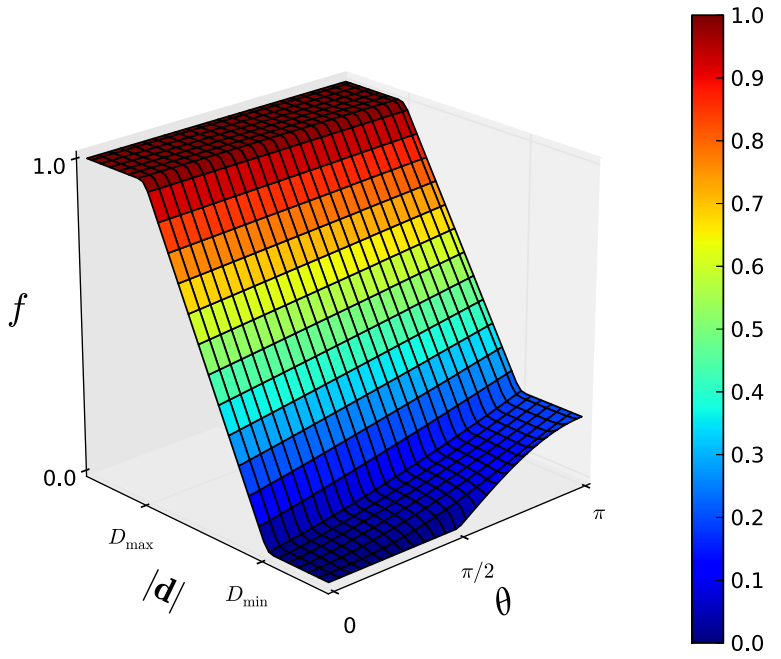

Figure 3.6: Graph of the function f with $F_{\text{rec}} = 0.2$.

follows:

$$r(d_{jh}) = (1 - \frac{F_{\text{rec}}}{2}) \frac{d_{jh} - D_{\text{min}}}{D_{\text{max}} - D_{\text{min}}} + \frac{F_{\text{rec}}}{2}, \tag{3.3a}$$

$$r'(d_{jh}) = \frac{F_{\text{rec}}}{2} \frac{D_{\text{max}} - d_{jh}}{D_{\text{max}} - D_{\text{min}}}. \tag{3.3b}$$

We introduce a recovery factor F_{rec} which is a constant to allow the robot to move slowly away from the human; thus a typical value of F_{rec} is for example 0.2. F_{rec} defines the minimum diameter of the auxiliary circle, which allows to recover the distance between human and robot. Figure 3.6 shows an example of the graph of f with a recovery factor $F_{\text{rec}} = 0.2$.

With the auxiliary circle, we can obtain speed restrictions for any direction of the motion, as shown in Figure 3.7.

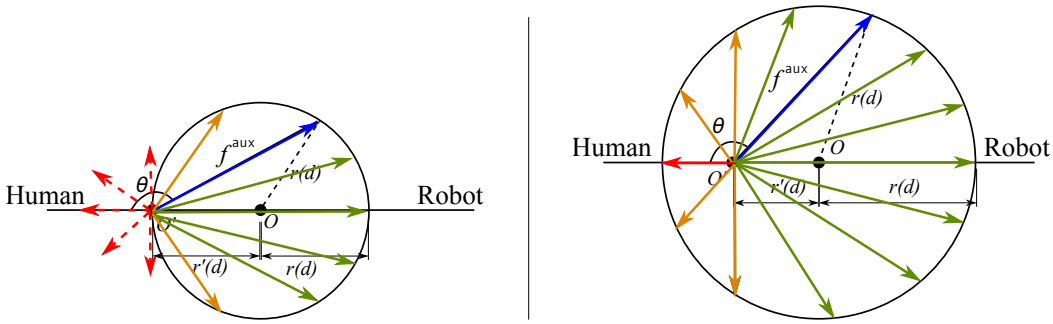

(a) $||\mathbf{d}|| \leq D_{\min}$ (b) $D_{\min} < \|\mathbf{d}\| < D_{\max}$

Figure 3.7: Speed restrictions for any direction of the motion using the auxiliary circle.

3.1.3 Algorithm

The AVM algorithm takes an original trajectory $\mathbf{q}(t)|t \in [0, T_{\text{end}}]$ as an input, and is executed at each time step Δt until $\mathbf{q}(t)$ is completed. AVM outputs the target joint angles $\mathbf{q}^*$ at each Δt according to the velocity restriction. The temporal remapping is done by calculating a *trajectory scaler* $s \in [0, 1]$ that indicates the degree of velocity modification; when $s = 1$ the robot will move at the original speed, and when $s = 0$ the robot will stop. An *internal time* $\tilde{t}$ is tracked to preserve the trajectory shape. We start with $\tilde{t} = 0$. At each Δt, $\tilde{t}$ is incremented by $s\Delta t$.

For every combination of points on the robot $j \in \{1, \ldots, m\}$ and points on the human body $h \in \{1, \ldots, n\}$, the trajectory scaler s_{jh} is computed. In this computation, we first obtain the speed limitation v_{jh}^{limit} from the linear velocity V_j of the original trajectory at the point j and the displacement d_{jh} (a vector from j to h). The scaler s_{jh} is obtained from v_{jh}^{limit} so that the actual speed does not exceed v_{jh}^{limit}. Finally, we choose the most strict scaler $\hat{s}$ (i.e., the smallest) from s_{jh}. We treat $\|\mathbf{V}_j\| = 0$ (i.e., j is not moving) as a special case, where the scaler is $s_{jh} = 1$ for every h.

Algorithm 1 shows the entire computation at each time step. The current joint angles are denoted by $\mathbf{q}_{\text{curr}}$, V_{safe} denotes a constant speed limitation for any

Algorithm 1: Asymmetric Velocity Moderation

Input: Δt, $\mathbf{q}(t)|t \in [0, T_{\text{end}}]$, $\mathbf{q}_{\text{curr}}$, $\tilde{t}$, $\{\mathbf{d}_{jh}|j \in \{1,\ldots,m\},\ h \in \{1,\ldots,n\}\}$

Output: $\mathbf{q}^*$, $\tilde{t}$

Get the original target joint velocity:

$$\dot{\mathbf{q}} \leftarrow \frac{\mathbf{q}(\tilde{t} + \Delta t) - \mathbf{q}_{\text{curr}}}{\Delta t}$$

for each robot point j **do**
  Calculate velocity $\mathbf{V}_j \leftarrow \mathbf{J}_j(\mathbf{q}_{\text{curr}})\dot{\mathbf{q}}$
  for each human link h **do**
    if $\|\mathbf{V}_j\| = 0$ **then**
      $s_{jh} \leftarrow 1$
    else
      $d_{jh} \leftarrow \|\mathbf{d}_{jh}\|$
      $\theta_{jh} \leftarrow \cos^{-1}\left(\frac{\mathbf{d}_{jh} \cdot \mathbf{V}_j}{\|\mathbf{d}_{jh}\|\|\mathbf{V}_j\|}\right)$
      $v_{jh}^{\text{limit}} \leftarrow f(d_{jh}, \theta_{jh}) V_{\text{safe}}$
      $s_{jh} \leftarrow \min\left(\frac{v_{jh}^{\text{limit}}}{\|\mathbf{V}_j\|}, 1\right)$
    end if
  end for
end for
$\hat{s} = \min(s_{jh})$
$\mathbf{q}^* \leftarrow \mathbf{q}(\tilde{t} + \hat{s}\Delta t)$
$\tilde{t} \leftarrow \tilde{t} + \hat{s}\Delta t$

situation[4], f is a function to compute v_{jh}^{limit}, and $\mathbf{J}_j(\mathbf{q})$ denotes the Jacobian of the point j at joint angles $\mathbf{q}$.

Note that the AVM algorithm accepts any selection of representative points, so this selection can be changed according to the situation. In this work, for every combination of a point j on the robot's joints and a link h on the human, AVM computes the closest point on the link h from the point j. This point and the matching point j are then used as a pair of representative points. We consider these representative points as reasonable for articulated robots such as humanoid robots.

3.1.4 Discussion

In the proposed AVM algorithm, the human is assumed to be static at every frame because the human motion is not considered in the calculation. This is because the direction of the motion derives from the angle between the displacement vector and the robot velocity vector. During the interaction, both the human and the robot are responsible for the human safety. By assuming the human is static at each frame, we make the danger depend mostly on the robot behavior (at each frame). This aligns with the heuristic approach and this dissertation's philosophy that the robot should have bigger responsibility during the interaction.

Nevertheless, the AVM algorithm can be modified so that the human behavior is also considered by adding the human velocity. With the assumption that human is moving at each frame, the danger of the interaction is also influenced by the human behavior.

To achieve this, the calculation of the angle θ_{jh} (step 9 of the AVM algorithm) can be modified as follows:

$$\theta_{jh} \leftarrow \cos^{-1}\left(\frac{\mathbf{d}_{jh} \cdot (\mathbf{V}_h - \mathbf{V}_j)}{\|\mathbf{d}_{jh}\|\|\mathbf{V}_h - \mathbf{V}_j\|}\right), \tag{3.4}$$

where $\mathbf{V}_h$ is the velocity vector of a representative point on the human, and $\mathbf{V}_j$ is the velocity vector of a representative point on the robot.

[4] V_{safe} is a constant value, e.g., 250 mm s^{-1} as standardized in the ISO 10218 [15].

Summary

- The heuristic approach uses the human notion of danger to implement the control policy.
- AVM is a controller that restricts the robot speed according to distance and the direction of the motion to keep human safety.
- AVM restricts the robot speed more when moving toward the human and relaxes the restriction when moving away.
- The asymmetric restriction maintains the robot's performance while also keeping human safety.

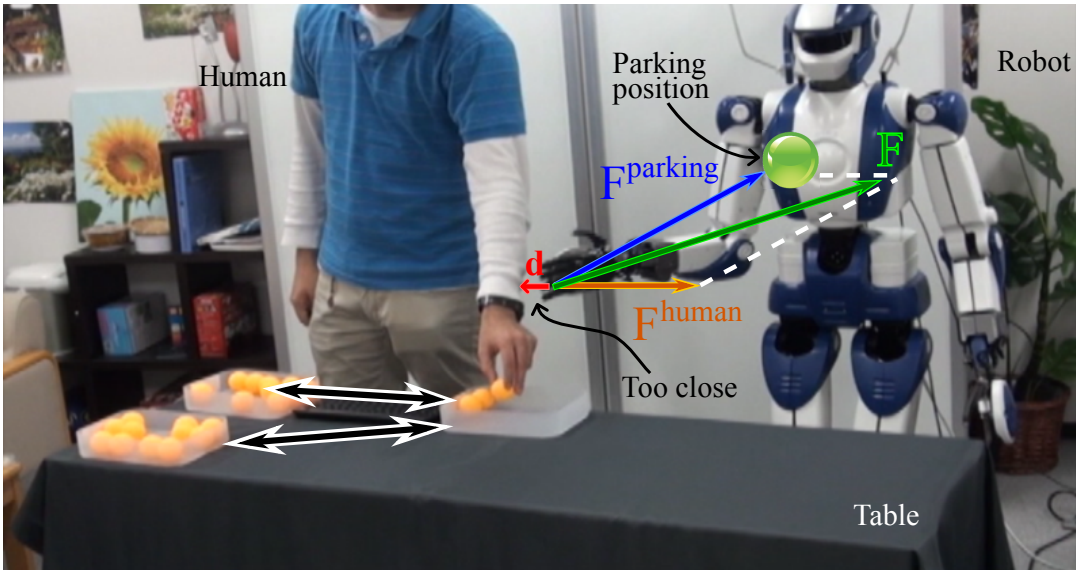

Figure 3.8: Virtual force $\mathbf{F}$ as the combination of $\mathbf{F}^{\text{human}}$ and $\mathbf{F}^{\text{parking}}$. The sphere indicates the parking position assumed to be safe.

3.2. Withdrawal strategy

This section introduces Withdrawal as a strategy whose purpose is to increase the distance from human when the robot is too close to the human. The motivation here is to show how the low-level controller AVM works with a higher-level controller, such as Withdrawal.

An actual use case of Withdrawal is when the human and robot are trying to reach a location in the same region. We use a virtual force model to modify the end-effector velocity and move it not only away from the human but also toward a predefined parking position, as shown in Figure 3.8. At all times, AVM is auditing the produced motions to guarantee human safety.

3.2.1 Phases of Withdrawal

Withdrawal pauses the robot's task by creating a temporal deviation from the original trajectory, increasing the distance from the human, and then going back to where it started to allow the robot to continue with the task.

Withdrawal has two phases: *TakeOut* and *PlaceBack*. *TakeOut* places the end-effector in a safer location. *TakeOut* starts when the distance to the human is too short and the restriction calculated by AVM is very high, i.e., the speed of the end-effector is almost zero. Once the end-effector has increased the distance to the human, the *PlaceBack* phase starts. *PlaceBack* moves the end-effector from the location achieved by *TakeOut* to the location where Withdrawal was engaged.

3.2.2 Virtual force model of Withdrawal

The virtual force model of Withdrawal was constructed using two virtual forces: a repelling force $\mathbf{F}^{\text{human}}$ exerted by the human, and an attractive force $\mathbf{F}^{\text{parking}}$ exerted by the parking position. This virtual force model is inspired by the Social Force Model (SFM), which describes the interactions between pedestrians using social forces [34].

As explained by Luber *et al.*, the Social Force Model can describe the interactions between pedestrians by making use of social forces [35]. Such forces aim to model the behavior of the human motion, which is considered to be affected by the motion of other humans and the environment. Therefore, these forces may be derived from the motivation of the human to reach his goal, the repulsive effect of obstacles, physical constraints, and so on.

Luber *et al.* define the social forces as follows:

$$\mathbf{f}_{i,k}^{\text{soc}} = a_k \exp\left(\frac{c_{i,k} - d_{i,k}}{b_k}\right)\boldsymbol{n}_{i,k} \tag{3.5}$$

where i is the index of the human receiving the influence of the force, k is another human or an object, a_k represents the magnitude of the force, and b_k denotes the range of the force. Since humans and objects are represented as circles, c_i and c_k are the radius of the human i and the radius of the human or object k that is exerting the force. $c_{i,k}$ is the sum of these radii and $d_{i,k}$ is the distance between the centers of the circles. Finally, $\boldsymbol{n}_{i,k}$ is a normalized vector that points from the human or object k to the human i.

Even though the Social Force Model was originally developed to address the interaction between pedestrians, it can be modified to be applicable to other cases not only involving human-human interaction but also HRI. This is due to the fact

that the core concept of the Social Force Model is to use virtual forces to model the behavior of human motion and its relations with the environment, whether if such environment is populated by other humans or robots.

Like previous modifications of SFM [36, 37], we modify the SFM so that the contributions of $\mathbf{F}^{\text{human}}$ and $\mathbf{F}^{\text{parking}}$ are summarized in a resulting force $\mathbf{F}$, which is used to change the end-effector velocity.

$\mathbf{F}^{\text{human}}$ derives from human proximity, so it increases proportionally to the distance to its source, i.e., the minimum distance between human and robot:

$$\mathbf{F}^{\text{human}} = M\exp\left(\frac{-d}{R}\right)\mathbf{n}, \tag{3.6}$$

where M and R represent the magnitude and range, and d is the minimum distance. The vector $\mathbf{n}$ is obtained by normalizing the displacement vector but reversing its direction, i.e., from the human to the robot.

$\mathbf{F}^{\text{parking}}$ attracts the end-effector to a fixed position, where we assume it is safe to park the end-effector.

$$\mathbf{F}^{\text{parking}} = A\mathbf{p}, \tag{3.7}$$

where A is the magnitude and $\mathbf{p}$ is the normalized vector pointing from the current location of the end-effector to the parking position. We set $\mathbf{F}^{\text{parking}}$ as a constant force to make the end-effector converge to the parking position.

Finally, the motion of the end-effector is calculated as $\frac{\mathrm{d}}{\mathrm{d}t}\mathbf{V} = \frac{\mathbf{F}}{m}$, where $\mathbf{F}$ is the sum of $\mathbf{F}^{\text{human}}$ and $\mathbf{F}^{\text{parking}}$, m is the human mass, and $\mathbf{V}$ is the resulting end-effector velocity.

Summary

- Withdrawal is a reflexive response to avoid collisions.
- The achieved reflex resembles the human motion when withdrawing his arm if another human is trying to reach the same region simultaneously.
- This strategy increases the distance to the human using a virtual force model which moves the end-effector away from the human and towards a safer location.

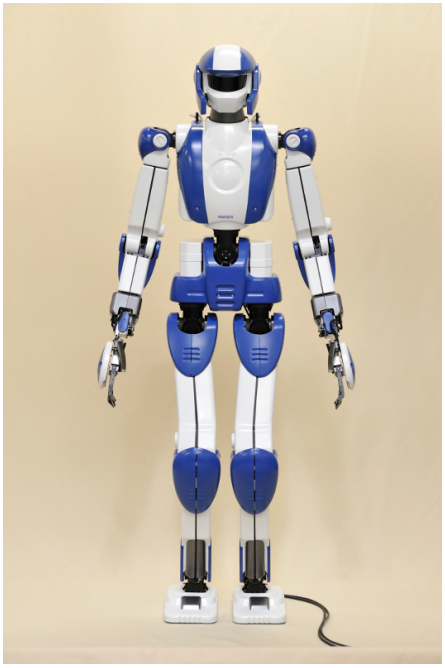

Figure 3.9: Humanoid robot HRP-4. This humanoid manufactured by Kawada Industries is 151 cm high, weights 39 kg, and has 34 DOF.

3.3. Experimental setup

This section describes the testbed and sensors used for the simulation and real-robot experiments. Moreover, the compared methods, four test cases for human safety comparison and eight HRI scenarios for efficiency evaluation are introduced. The difference between the test cases and the HRI scenarios is that the test cases are short motion sequences where the robot undoubtedly endangers the human, while the HRI scenarios are intended for longer interactions similar to those found in daily-life environments.

3.3.1 Test bed

The experiments are carried out using a humanoid robot and human subjects. We use the humanoid robot HRP-4 introduced by Kaneko *et al.* [38], shown in Figure 3.9. As shown in Figure 3.10, we place a table in front of the subject on

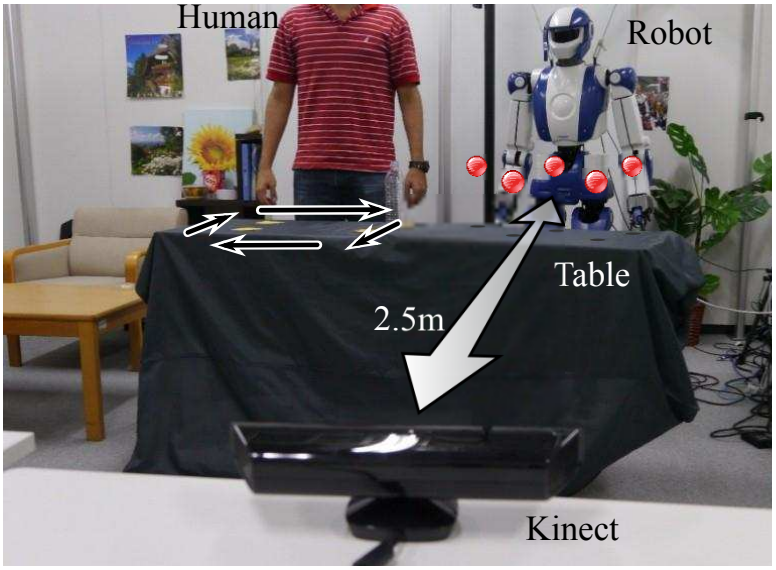

Figure 3.10: Experimental setup with a humanoid robot and a human subject. The spheres indicates the target positions of the humanoid task. The small arrows indicate the human task (moving a bottle among four destinations).

which both the human and robot perform their tasks.

We measure the state of the human subjects using either an RGB-D sensor or a *sensor suit*. The RGB-D sensor is a Microsoft Kinect sensor. Even though using an RGB-D sensor is relatively simple, this kind of sensors has occlusion problems that makes it suitable only for scenarios where the human and robot are facing the sensor. The sensor suit is the inertial motion capture system Xsens MVN[5], shown in Figure 3.11. Using the sensor suit we obtain the 3D position of 23 joints of the human body.

To visualize the human and robot motions and their whole-body relationship We use a virtual environment implemented using the 3D engine Irrlicht[6], shown in Figure 3.12. We implemented AVM using the OpenRTM[7] platform described by Chen *et al.* [39]. For the Microsoft Kinect sensor, we use the *Kinect for Windows SDK* version 1.5 and for the sensor suit, we use the MVN SDK version

[5]Xsens MVN inertial motion capture system manufactured by Xsens Technologies B.V.
[6]"Irrlicht Engine," `http://irrlicht.sourceforge.net` .
[7]"OpenRTM-aist," `http://www.openrtm.org` .

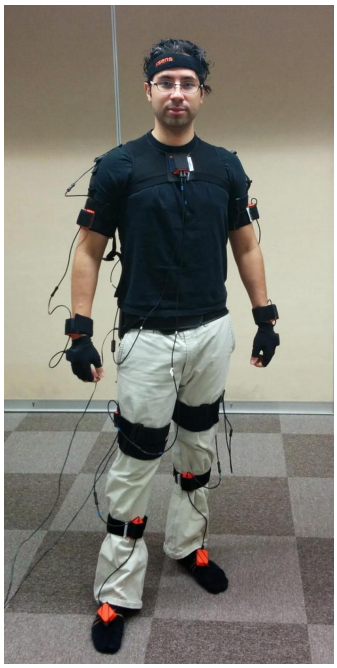

Figure 3.11: Human subject wearing the sensor suit. Each of the sensors integrates 3D magnetometers measuring the Earth magnetic field, 3D linear accelerometers measuring accelerations including gravitational acceleration, and 3D rate gyroscopes measuring angular velocities.

2.6. The trajectories of the robot task are generated using OpenRAVE[8] library version 0.9 developed by Diankov [40].

Even though AVM performs a better assessment of human safety when considering multiple displacement vectors distributed along the human and robot bodies, AVM can also work with limited information such as only the closest point. This increases the applicability of the proposed algorithm to cases where segmentation of the human body into links is not possible, such as the case where an RGB-D sensor provides only voxel information of the whole bodies.

[8]Diankov, R.: "OpenRAVE," `http://www.openrave.org` .

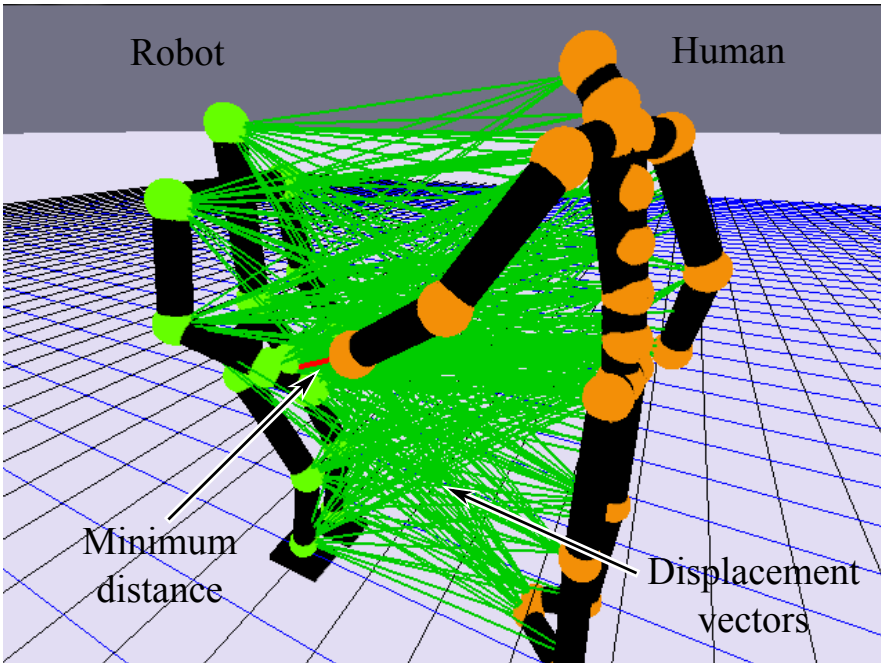

Figure 3.12: Virtual environment used for the simulation experiments.

3.3.2 Distance calculation

To calculate the distance with the sensor suit, we create two models: a human model from the joint positions obtained with the sensor suit, and a robot model from forward kinematics. The joints of both human and robot are modeled as spheres while the links between the joints are modeled as cylinders. We calculate the distance analytically by using the geometric properties of the spheres and cylinders.

To calculate the distance with the Microsoft Kinect sensor, we use the depth information. The Kinect SDK detects the human and robot voxels from which we calculate the minimum distance, as shown in Figure 3.13. This is a *bichromatic closest pair of points* problem, as described by Agarwal *et al.* [41]. We solve it by converting one of the sets to a k-d tree [42] and then performing a nearest neighbor search [43].

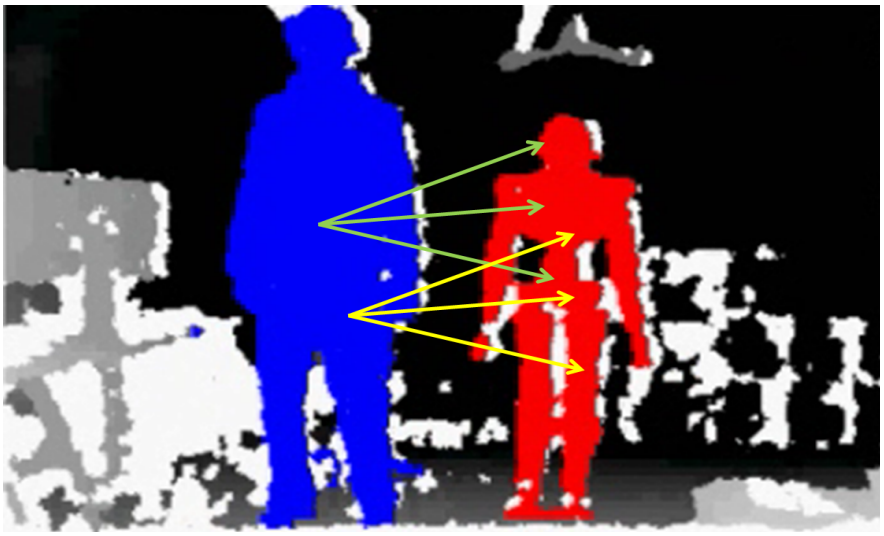

Figure 3.13: Distance calculation from voxel information.

3.3.3 Compared methods

We compare the effect of the following methods on human safety and the robot's efficiency:

M-1. Conventional method which separates the human and the robot during the interaction by stopping the robot every time the human enters the robot's workspace ($d_{jh} < D_{\max}$). This method generates a partial isolation from the human since it considers the human enters its workspace when the distance between the closest points is less than $D_{\max}$, as opposed to a total isolation where a distance from the robot base to any point on the human is used (e.g., a fence). Therefore, the conventional method used in this dissertation allows a closer interaction than a conventional method using a fence.

M-2. This method restricts the robot speed based only on distance, i.e, the direction of the motion is neglected. The restriction is calculated as $\frac{d - D_{\min}}{D_{\max} - D_{\min}}$ for $D_{\min} \leq d \leq D_{\max}$.

M-3. A special case of AVM that calculates the speed restriction based on distance, and the closest point and its velocity.

M-4 (proposed). AVM calculates speed restrictions for every combination of robot joints and human links.

(No method). This is a reference to compare the above listed methods to the case where no safety method is applied and no human is present, i.e., the robot moves freely.

By comparing M-1 to M-2, we demonstrate the improvement in the efficiency and how using the closest point allows a closer HRI. By comparing M-2 to M-3, we validate the positive effect of the asymmetry of AVM on the robot's efficiency without risking human safety. Finally, by comparing M-3 to M-4 (proposed), we show that considering multiple points on human and robot leads to a better assessment of human safety, which allows an even closer HRI.

Figure 3.14 shows a representation of the restriction for each method.

3.3.4 Test cases

We use four test cases to verify AVM in terms of safety. These test cases derive from possible dangerous situations that humans may encounter in daily-life scenarios, similarly to those found in the work of Haddadin *et al.* [44] and Malm *et al.* [45].

TC-1. The robot is bending its arm while the human has his arm right next to the robot's elbow. In this dangerous situation, the human arm gets crushed by the robot.

TC-2. The robot moves its arm toward the human body. In this dangerous situation, the robot approaches the human body. Here, the closest point does not correspond to the fastest point on the robot, which could cause greater damage.

TC-3. The robot turns its body toward the human. In this dangerous situation, the robot collides with the human when turning.

TC-4. The human has his arm bent 90 degrees. The robot moves its right arm parallel to the upper arm of the human and hits the forearm.

The test cases TC-1 to TC-4 are shown in Figures 3.15(a) to 3.15(d), respectively.

3.3.5 Simplified HRI scenarios

To verify the performance of AVM, we use eight experimental setups which depict simplified HRI scenarios where a humanoid robot could endanger a human, shown

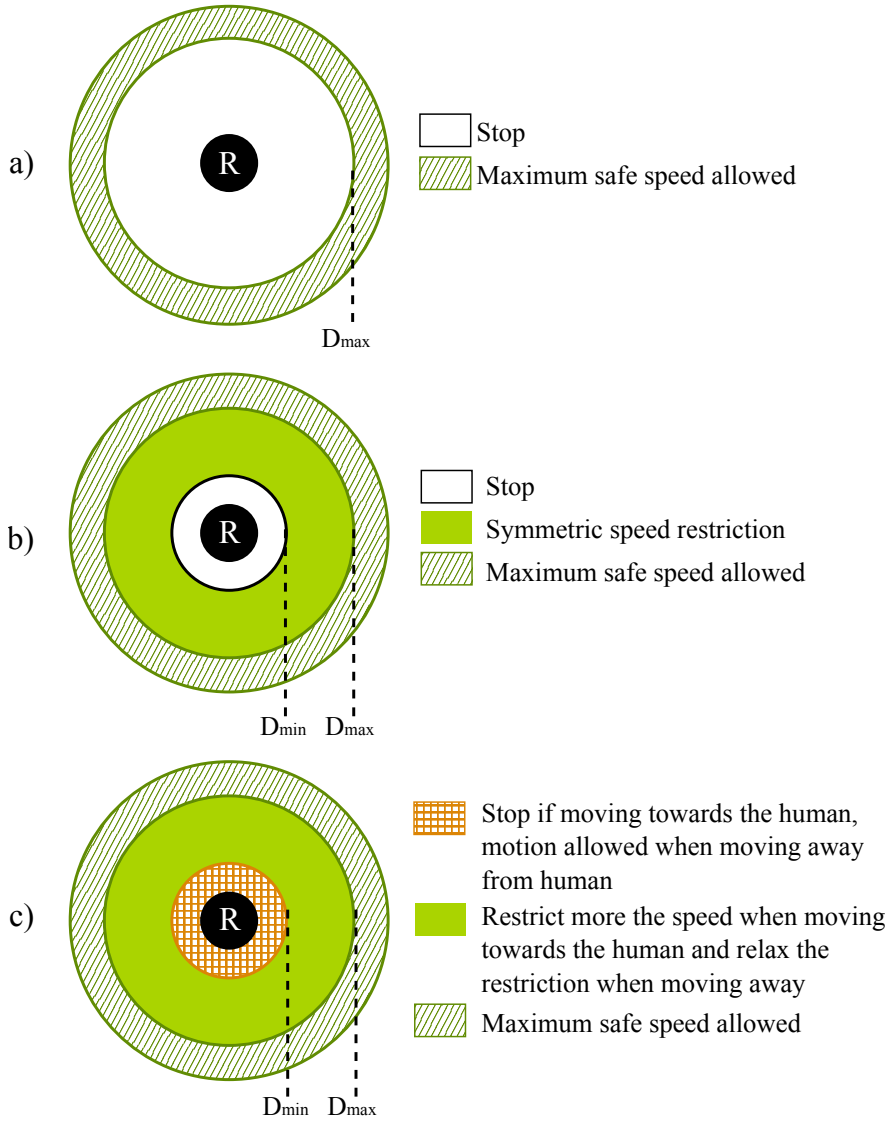

Figure 3.14: Representation of the speed restriction of the compared methods. (a) corresponds to M-1, (b) to M-2, and (c) corresponds to M-3 and M-4. The difference between these last two is that M-3 uses only the closest points while M-4 applies this concept to multiple points on both the human and robot (R). D_{min} and D_{max} are the distance thresholds.

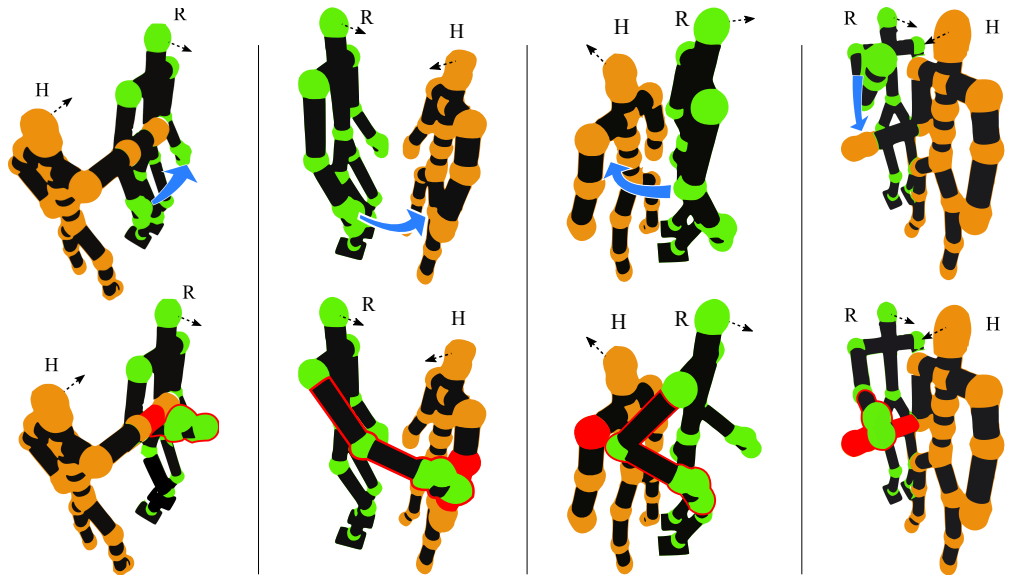

(a) TC-1 (b) TC-2 (c) TC-3 (d) TC-4

Figure 3.15: Schematics of the test cases for the human safety comparison. The upper figures show the initial state while the bottom figures show the collision state. The thick arrows show the direction of the robot's motion. The dotted arrows indicate the facing direction of the human and robot.

in Figure 3.16. We selected these scenarios considering what we envision could be common situations in daily-life scenarios where a robot performs a task in human proximity. The locations and orientations depicted by these scenarios mimic those found in daily life environments such as a house or an office.

We place both human and robot around a table (70 cm high). The separation between the right feet of the human and robot in each scenario is approximately 76 cm (scenarios 1 and 2), 78 cm (scenarios 3 to 6), 49 cm (scenario 7), and 67 cm (scenario 8), respectively. In scenario 1, human and robot are facing the same direction, while in scenario 2 they are facing each other. In scenarios 3 and 4, the human is in front of the robot but rotated 45 degrees to the left and right, respectively. Similarly, in scenarios 5 and 6 the human is rotated 90 degrees to the left and right, respectively. In scenario 7, human and robot are back to back. Finally, in scenario 8, human and robot are facing in opposite direction and one

Figure 3.16: Simplified HRI scenarios with a humanoid (R) and a human subject (H) performing independent tasks. The circles indicate the five different positions above the table where the robot can place the end-effector. The rectangles are the boxes among which the human subject moves objects. The moving links are indicated in solid color.

to the right of the other.

Human and robot perform independent tasks around the table. The task of the human consists of moving balls between three boxes on a table. The task of the robot consists of placing the end-effector 30 times in different positions on the table, chosen randomly out of five predefined positions. The circles in Figure 3.16 indicate these five different positions, which are on the same plane about 20 cm above the table and are reachable by the robot.

By using a metronome, the human movement between boxes was conditioned to be completed in 1 s. This limitation is to ensure that the human does not intentionally move away from or toward the robot, which could introduce a bias in the task completion time. Since in some robot configurations with the con-

ventional method (M-1) the robot was not able to continue its task, the time is pruned to a maximum of 400 s.[9] The maximum allowable speed $\mathbf{V}_{\text{safe}}$ is set to 250 mm s^{-1}, as standardized in the ISO 10218 [15]. The distance thresholds D_{min} and D_{max} are set to 100 mm and 300 mm, respectively. Finally, the recovery factory F_{rec} is set to 0.2.

Summary

- The test bed consists of the humanoid robot HRP-4, an RGB-D camera, and a motion capture system.
- For the experiments, we use four test cases which are *a priori* dangerous situations.
- Also, we use eight HRI scenarios similar to those found in daily life where human and robot are next to each other and a table.
- The task of the robot is to randomly move the end-effector above the table.
- The task of the human is to move objects on the table.

[9] Considering that the mean of the simulation experiments is 163 ± 53 s.

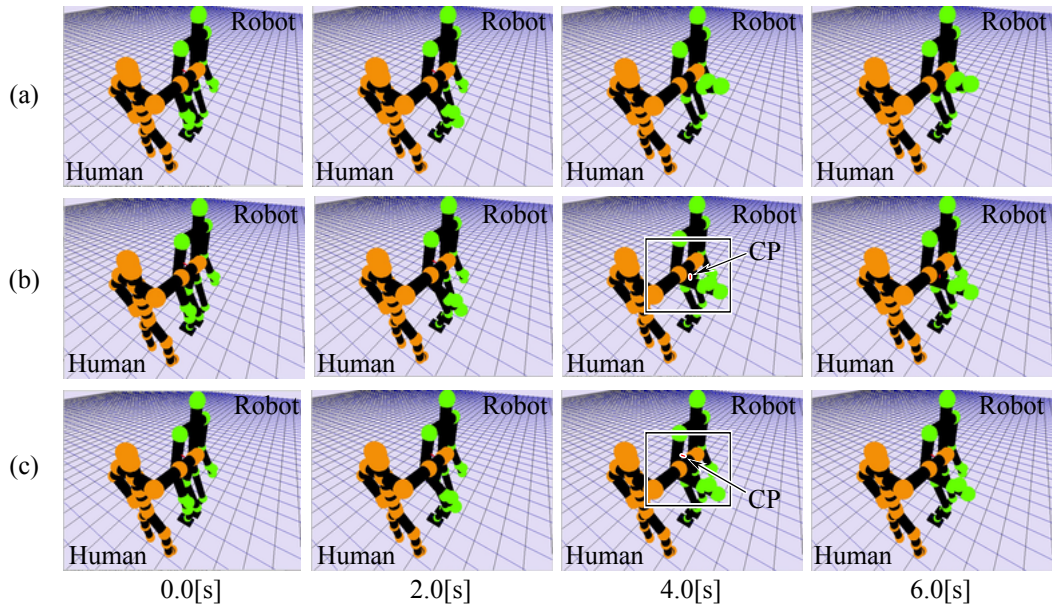

Figure 3.17: Screenshots of test case TC-1. Row (a) shows the collision that would occur if no method is used. Rows (b) and (c) show the resulting configurations using M-3 and M-4 (proposed), respectively.

3.4. Experimental results

In this section, we compare four methods in terms of a) human safety by simulating dangerous situations, and b) efficiency using eight HRI scenarios, both with simulation and real-robot experiments.

3.4.1 Simulation

The objective of the simulation experiments is to test situations which are known to be dangerous. Moreover, we test the robot behaviors with a recorded human motion to verify the human safety and the robot's efficiency.

Human safety comparison

As detailed below, the robot performs a better assessment of human safety when using multiple displacement vectors, in contrast to using only the closest point.

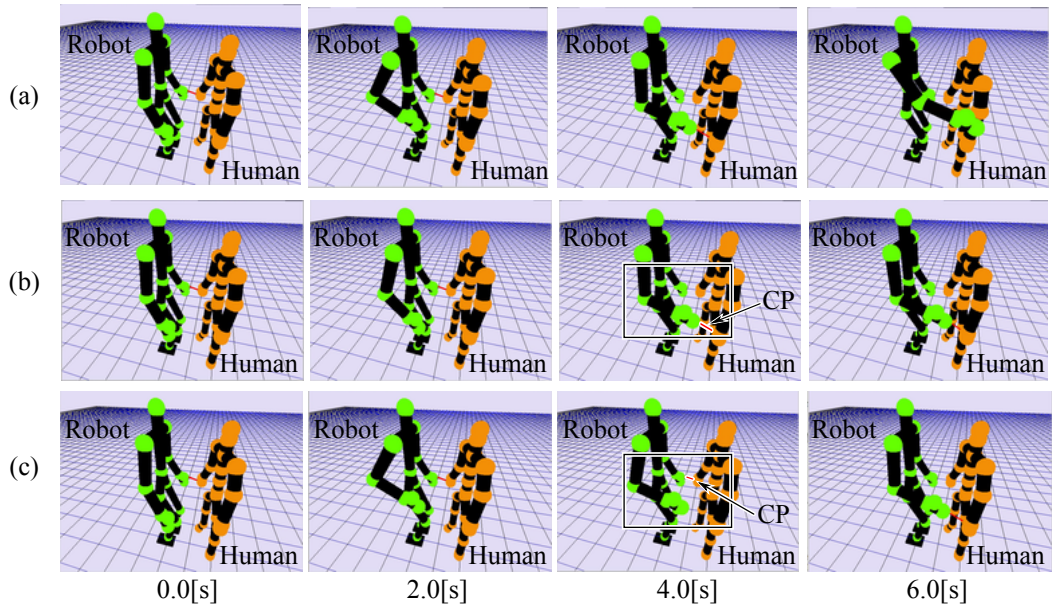

Figure 3.18: Screenshots of test case TC-2. Row (a) shows the collision that would occur if no method is used. Rows (b) and (c) show the resulting configurations using M-3 and M-4 (proposed), respectively.

This translates into a smoother decrease in the speed along with earlier prevention of a possible collision.

Figures 3.17 to 3.20 show the screenshots of the test cases TC-1, TC-2, TC-3, and TC-4, respectively. Row (a) shows a collision with the human since no method was used to restrict the robot. Rows (b) and (c) show the results of M-3 and M-4, respectively. The screenshots of M-1 and M-2 are omitted since with these methods the robot is not able to approach the human. Figures 3.21 to 3.24 show the speed profiles of the end-effector for each test case.

In TC-1, when using M-3, the robot approaches the human rapidly because the speed is not firmly restricted until the closest point is on the forearm. As shown in Figure 3.17, when using M-4 (proposed), the robot better estimates the risk of crushing the human and stops earlier. As shown in Figure 3.21, using this method, the robot gradually reduces its speed and keeps farther from the human than when using only the closest point.

In TC-2, when using M-3, the robot approaches the human rapidly because

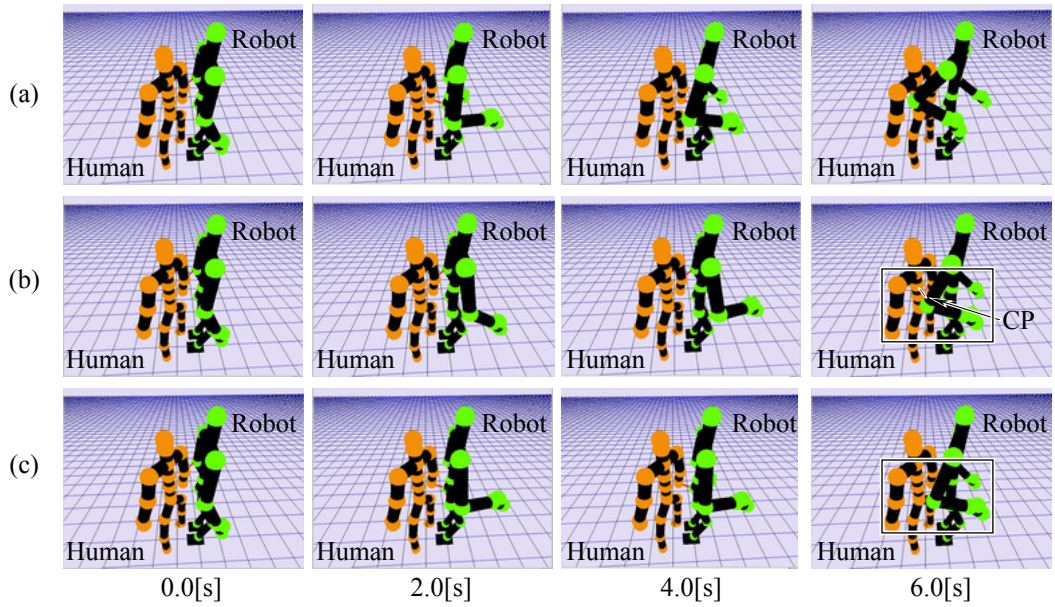

Figure 3.19: Screenshots of test case TC-3. Row (a) shows the collision that would occur if no method is used. Rows (b) and (c) show the resulting configurations using M-3 and M-4 (proposed), respectively.

the closest point lies on a non-moving joint. When the closest point changes to the approaching joint (Figure 3.18), the robot decreases its speed abruptly (Figure 3.22). When using M-4 (proposed), the robot considers the restrictions derived from other joints as well as the closest point, so it anticipates the risk of colliding with the human and stops earlier.

In TC-3, similarly to the previous cases, when using M-3, the robot underestimates the situation and turns rapidly toward the human. As shown in Figure 3.19, when using M-4 (proposed), the closest point remains away from the point where the collision occurs when no safety method is enforced. With this method, the robot is able to correctly estimate the situation and smoothly decrease the speed, as shown in Figure 3.23.

Finally, in TC-4, when using M-3, the robot stops just when the closest point is on the human forearm. When using M-4 (proposed), the robot manages to decrease its speed gradually. As shown in Figure 3.20, when the closest point to the end-effector is on the upper arm M-4 (proposed) does not consider that point as

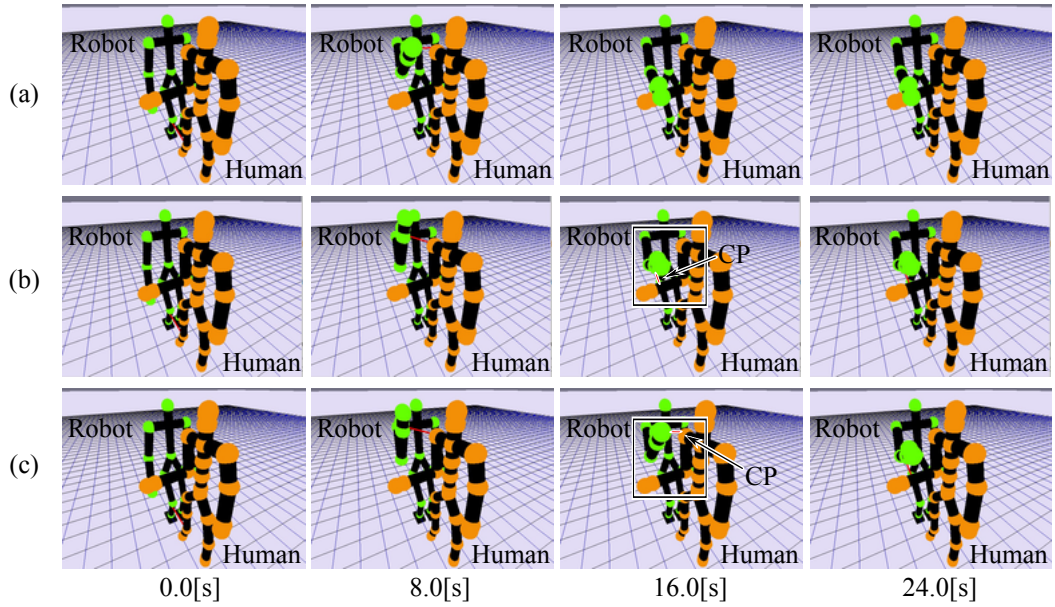

Figure 3.20: Screenshots of test case TC-4. Row (a) shows the collision that would occur if no method is used. Rows (b) and (c) show the resulting configurations using M-3 and M-4 (proposed), respectively.

the most dangerous point associated with the end-effector. M-4 (proposed) also calculates a restriction for the displacement vector formed by the end-effector and its closest point to the forearm. This makes the robot better assess human safety and correctly estimate the risk of a direct impact to the forearm. Figure 3.24 shows how M-3 keeps increasing the end-effector speed and then it abruptly reduces its speed when the closest point lies on the forearm. This figure also shows that M-4 (proposed) accounts for such situations and correctly reduces the risk of a direct impact to the forearm.

Efficiency evaluation

We perform simulation experiments by executing each method 10 times for each setup. In Figure 3.25, we present the task completion times of the compared methods, to evaluate the robot's efficiency.

As shown in Figure 3.25, in all of these cases with robot and human very close most of the time, M-1 produces an unnecessary severe speed restriction,

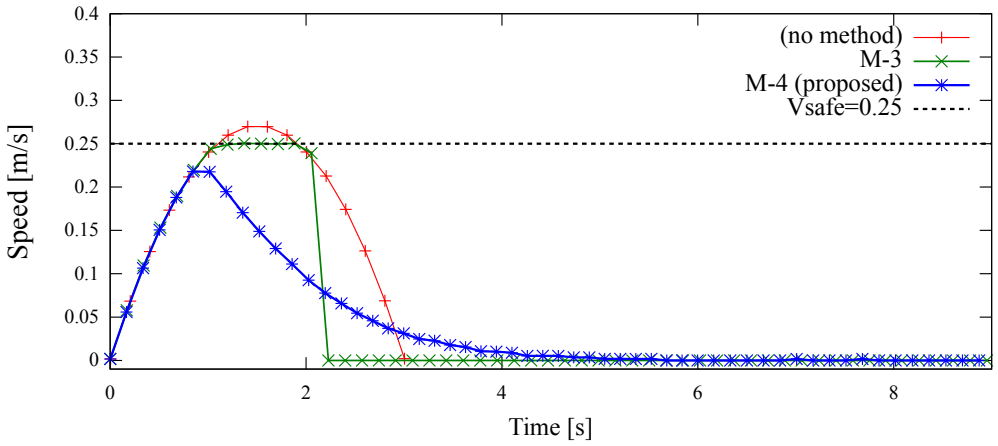

Figure 3.21: TC-1 speed profiles (end-effector).

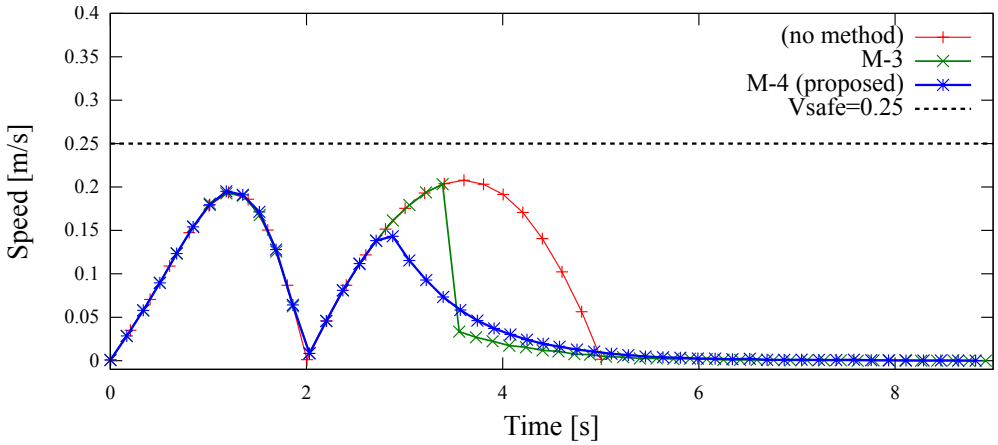

Figure 3.22: TC-2 speed profiles (end-effector).

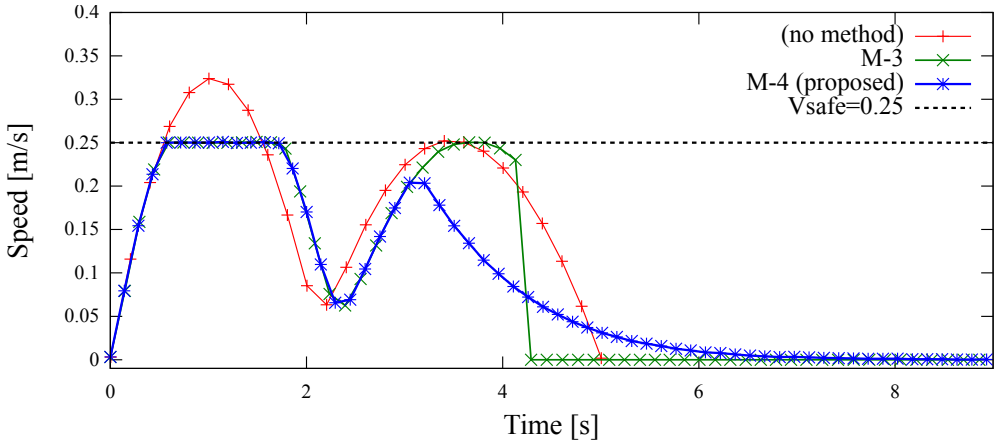

Figure 3.23: TC-3 speed profiles (end-effector).

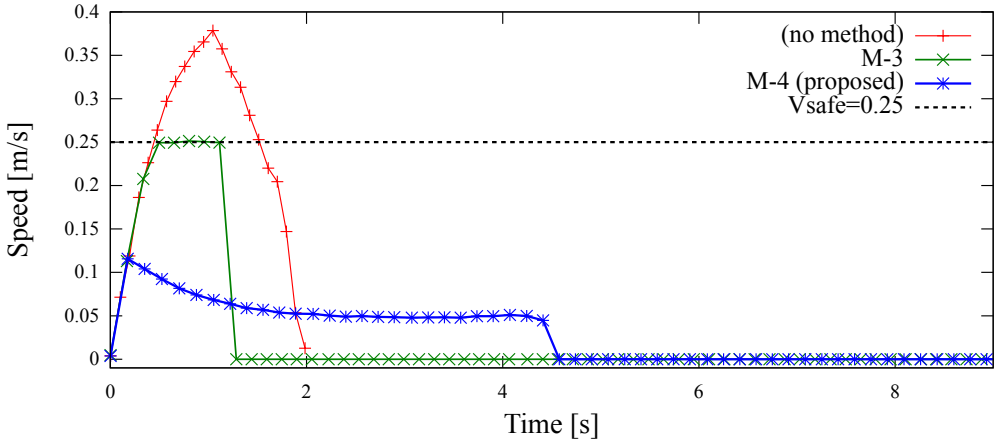

Figure 3.24: TC-4 speed profiles (end-effector).

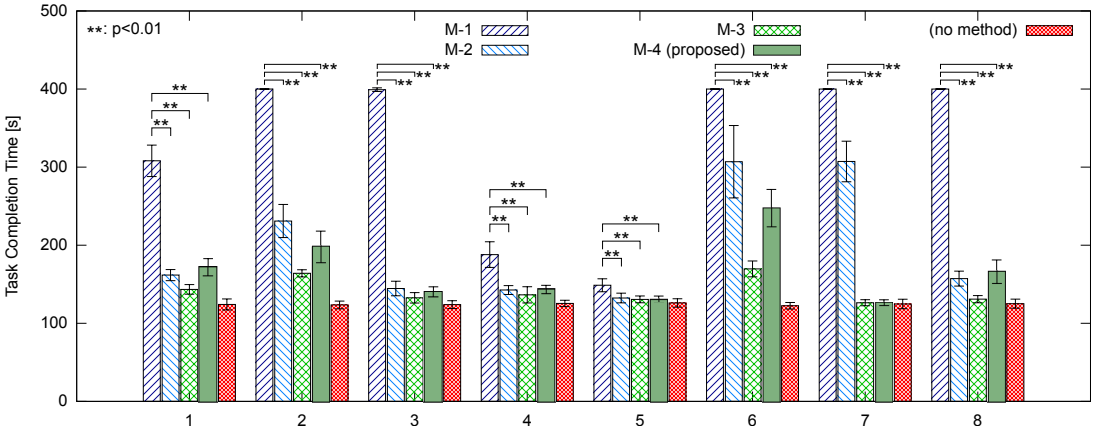

Figure 3.25: Simulation results. Task completion time corresponding to the setups 1 to 8. Lower is better.

negatively affecting the robot's efficiency. In most setups, M-3 produces better efficiency because it allows the robot to rapidly approach the human body. As can be seen in the figure, for setups 1, 2, 6, and 8, M-3 has significantly better task completion time than M-4 (proposed). This is because M-3 overestimates human safety by incorrectly assuming that the closest point is the most dangerous point. This endangers the human by allowing a faster motion than when using M-4 (proposed), as shown in Figures 3.21 to 3.24 where the speed of M-3 exceeds the speed of M-4. Finally, setup 7 especially shows the benefit of the asymmetry in AVM.

3.4.2 Real robot

In this section, we present the results of the experiments performed with the humanoid robot HRP-4 and 11 human subjects.

As this dissertation does not focus on the perception problem, we use the Microsoft Kinect sensor or the sensor suit to simplify the problem of obtaining the human state during the experiments. However, AVM is very general in terms of the human body model. Therefore, we can easily extend the human model to partially observable models.

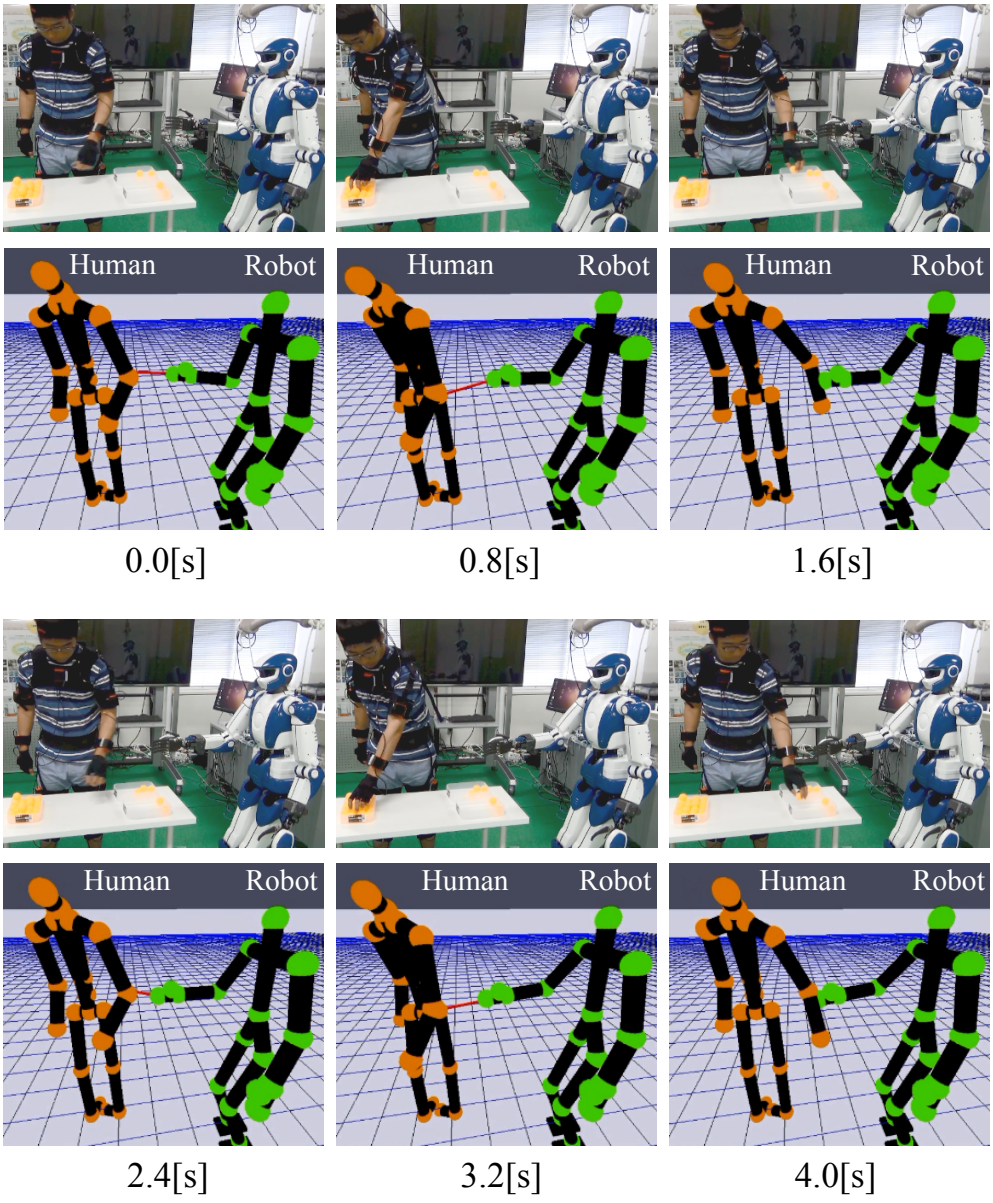

Figure 3.26: Screenshots of the experiments with the humanoid robot HRP-4 and a human subject wearing the sensor suit manufactured by Xsens Technologies B.V.

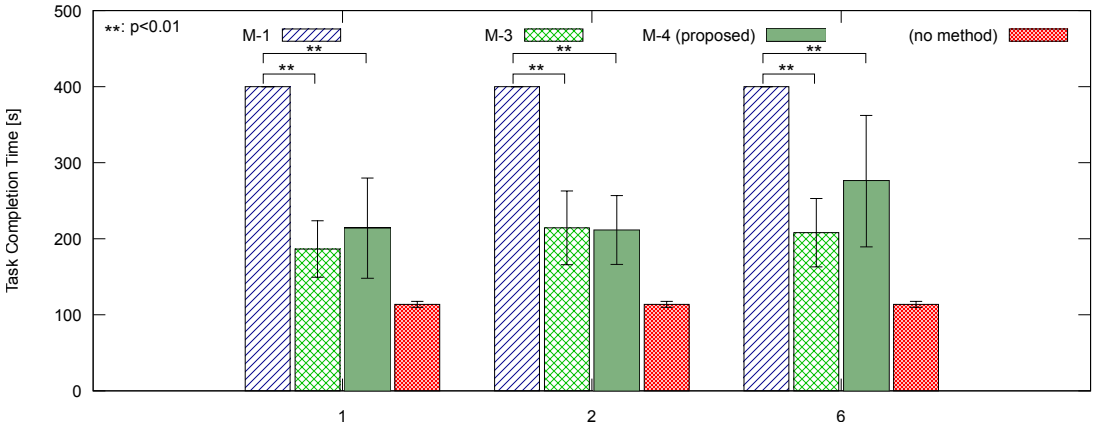

Figure 3.27: Real-robot results. Task completion time corresponding to the setups 1, 2 and 6 obtained with the HRP-4 robot and the sensor suit. Lower is better.

Simplified HRI scenarios

The experiments consist of having the robot complete its task in human proximity, using one method and one scenario at the time. Six human subjects participate in the experiments (men from 23 to 30 years old).

We perform experiments with the HRP-4 and human subjects wearing the sensor suit, as shown in Figure 3.26. We selected setups 1, 2 and 6 for the real-robot experiments as they showed the most significant variations in terms of the task completion time during the simulation experiments. The task completion times of the setups 1, 2 and 6 obtained with the HRP-4 and the sensor suit are shown in Figure 3.27. The time of *no method* is measured without the subjects. The graphs show that the tendencies in the task completion times are similar to those obtained from the simulation. M-4 (proposed) provides a better assessment of human safety since it considers the whole-body relationship between the human and robot, as shown in Figures 3.21 to 3.24 where the speed of M-3 exceeds the speed of M-4 (proposed).

With AVM the robot is able to complete its task in less time than the conventional method (M-1). As AVM reduces the task completion time when moving away from the human, the efficiency of the robot improves. On the other hand, when the robot is moving toward the human, the efficiency of the robot is, at worst, similar to a non-asymmetric approach.

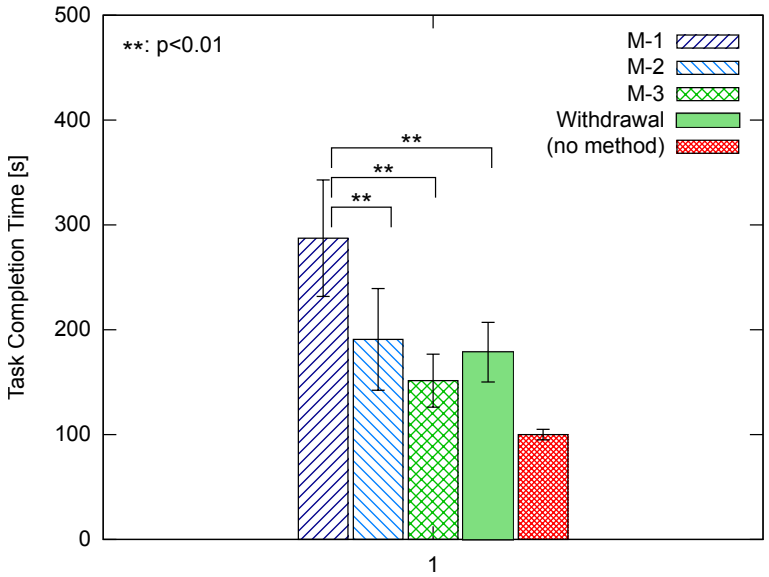

Figure 3.28: Real-robot results. Task completion time corresponding to the setup 1 obtained with the HRP-4 robot, the Microsoft Kinect sensor, and the Withdrawal strategy. Lower is better.

As shown in Figure 3.27, in setup 6, M-4 (proposed) is slower than M-3 because M-4 estimates the collision risk with the human hand while M-3 considers only the closest point, which most of the time lies on the elbow.

AVM as a low-level controller for human safety

We also validate AVM as a low-level controller for human safety using Withdrawal. The purpose of this experiment is to verify that AVM can guarantee human safety even though the target motion of the robot is generated without explicitly considering human safety. We implement Withdrawal to modify the robot behavior and test whether AVM is able to successfully restrict the generated motions in this situation.

We made the human and the robot perform simple tasks as in previous experiments. Withdrawal is engaged when the human and robot are trying to reach a location in the same region.

For these experiments, we use the M-3 method, the Microsoft Kinect sensor,

the humanoid robot HRP-4 and five human subjects (men from 23 to 30 years old). Due to the occlusion limitation of the RGB-D sensors, We only use setup 1 (i.e., with the human and the robot facing the sensor). The obtained task completion times are shown in Figure 3.28.

We verify that Withdrawal generates a deviation from the original trajectory and that this deviation is audited by AVM. We compare the absolute position of both the human and robot when using AVM only and when using Withdrawal, to observe the increase in distance between human and robot created by Withdrawal.

As shown in Figure 3.29, when using Withdrawal, if the human continues to come closer, the robot increases the distance to decrease the probability of a collision. This is in contrast with Figure 3.30, which shows that using AVM only results in just reducing the speed of the robot, leading to a shorter distance between human and robot with a higher probability of a collision. Even though Withdrawal generates a deviation from the original trajectory, driving the motion of the robot in a different way than initially intended, this motion is audited by AVM and ensured to be human-safe.

3.4.3 Discussion

AVM considers the distance and the direction of the motion to restrict the robot's speed. The whole-body relationship between human and robot is considered by calculating a speed restriction for every combination of human body parts and robot links. AVM proved to effectively generate human-safe motions to perform independent tasks in HRI scenarios. AVM is able to maintain human safety with a competitive robot's efficiency. Moreover, AVM works as a low-level controller auditing motions generated by behavior-specific strategies such as Withdrawal.

Withdrawal strategy increases the distance between human and robot when they are too close, in order to decrease the probability of a collision. This strategy creates a deviation from the original trajectory but keeps task completeness by returning to the configuration where it was engaged after distance was increased. The deviation depends on virtual forces which drive the end-effector through an unknown trajectory toward a parking position.

AVM is limited to observable human states which makes it purely reactive. At every frame, AVM captures the human state, evaluates human safety and

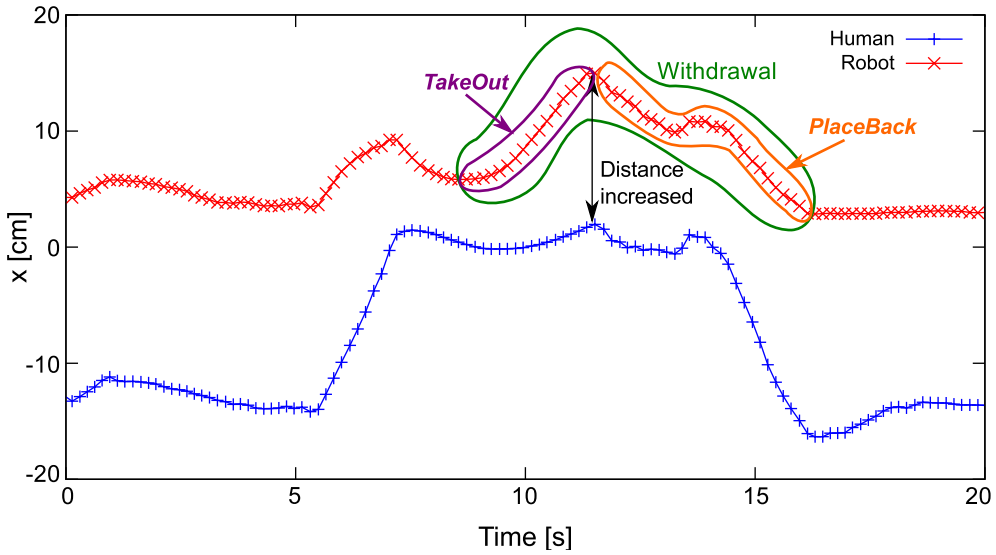

Figure 3.29: Plot of x coordinate of the absolute position of human and robot when using Withdrawal.

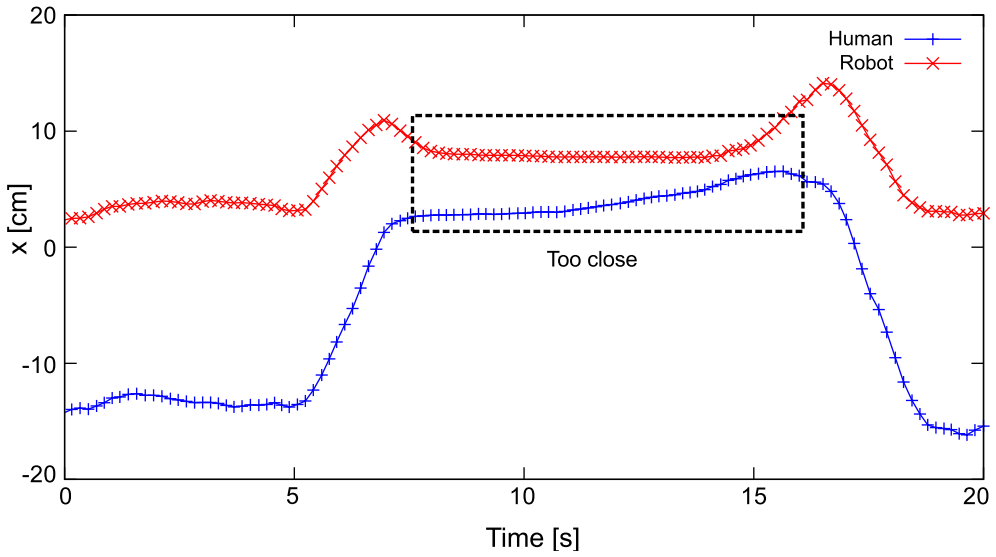

Figure 3.30: Plot of x coordinate of the absolute position of human and robot when using AVM only.

restricts the robot's speed accordingly. If the human motion can be estimated, future states can be used to evaluate human safety. Therefore, the robot's speed can be restricted earlier to further decrease the risk of a collision.

Summary

- The simulation experiments demonstrate that *a priori* dangerous situations can be handled by AVM and human safety can be guaranteed.
- We present a detailed analysis of human safety using AVM and the compared methods.
- AVM smoothly decreases the robot speed and keeps the human unharmed.
- In the real-robot experiments, AVM keeps the safety of the human subjects while they perform their tasks with the humanoid robot working in close proximity.
- We evaluate the robot's efficiency in terms of the task completion time.
- AVM has a competitive performance without sacrificing human safety.
- Withdrawal strategy effectively reduces the risk of a collision by increasing the distance to the human through a reflexive response.
- AVM supervises all the motions generated by Withdrawal to guarantee human safety.

Chapter 4

Analytical approach

This chapter describes an analytical approach to robot control for human safety. The motivation of this approach is to propose methods that are based on physical models rather than on the human notion of danger. This is because the human notion can underestimate the danger of situations which can be physically proven to be dangerous. The benefit of the analytical approach is a human safety assessment free of the danger underestimations inherent in the human notion, since it is supported by a physical analysis.

In this chapter, we propose a method to assess human safety where the consequence of a collision is integrated in the estimation of human safety. By considering how severe a collision is for the human, the robot behavior can be adapted to ensure that the human will not experience serious injuries should a collision occur. The severity of a collision derives from an analysis of physical quantities before and at the time of a collision.

The proposed human safety metric, or *safety index*, is a solution to the challenge of human safety assessment. Using distance and the direction of robot's motion as components of a safety metric has been proved to be effective to keep human safety, as described in Chapter 3. Nevertheless, this approach is not explicitly related to potential human injuries and is purely reactive. The proposed method associates the danger to potential human injuries by calculating the impact severity of a collision and anticipates the human motions to restrict the robot speed earlier, which decreases the risk of a collision. The novelty of the

proposed method consists of quantitatively evaluating human safety by modeling the human behavior so that it maximizes the potential injuries in a given situation.

Moreover, we develop a flexible controller capable of using multiple safety metrics in an interchangeable manner. This controller will make the robot move as fast as possible while complying with a human safety constraint. The potential benefit of this controller is that it can use existing safety metrics or newly released human safety standards, as it is independent from the safety metrics.

To test the proposed methods, simulation experiments are carried out where the human and robot do simple tasks in shared workspaces. The experimental results validate the proposed approach to guarantee human safety while keeping a competitive efficiency.

The rest of this chapter is organized as follows: Section 4.1 describes a novel metric to assess human safety which estimates the human behavior to anticipate the most dangerous situation. Section 4.2 introduces a controller capable of using different human safety metrics to ensure human safety. Finally, Section 4.3 presents the experimental results.

4.1. Safety Index

In this dissertation, the challenge of human safety is to control the robot in a safe and efficient way. Concretely, the problem can be described as assessing human safety given a state and a robot control input while satisfying a performance requirement. The assessment of human safety is given by a *safety index*, which is a scalar value that measures the safety of humans when interacting with a robot. This index provides a quantitative evaluation of human safety which can be used for robot control.

This section proposes a safety index to assess the human safety by considering the consequences of the most dangerous situation. The danger of a situation is derived from the potential injuries, i.e., the situation which could cause the most severe injuries is considered the most dangerous situation. Once we estimate the most dangerous situation, we can control the robot to avoid potential injuries which exceed acceptable limits.

The proposed safety index is based on a physical model to calculate danger, and a human model to predict the human motion. We rate the potential injuries according to the severity of a collision between human and robot. The severity of a collision derives from an analysis of physical quantities before and at the time of a collision. As an actual collision is undesired, we consider a collision between an estimated human state and a future robot state. To do this, we predict the human behavior from the observed human state and the human model, and calculate the future state of the robot from the control input.

The inputs of the safety index algorithm are the current human and robot states, which are defined by position and linear velocity, and the robot control input defined by the target velocity. The output is a numerical value associated to the impact severity of the worst human action, which represents the danger of the situation.

This section is organized as follows. Section 4.1.1 contains the details of the algorithm. Section 4.1.2 explains how danger is calculated. Section 4.1.3 details the human behavior estimation.

Algorithm 2: Safety Index

Input: $\mathbf{x}_{h0}$, $\mathbf{v}_{h0}$, $\mathbf{x}_{r0}$, $\mathbf{v}_r^*$
Output: SI

1: $\hat{\mathbf{a}}_h \leftarrow WHA(\mathbf{x}_{h0}, \mathbf{v}_{h0}, \mathbf{x}_{r0}, \mathbf{v}_r^*)$
2: $\mathbf{x}'_h \leftarrow \mathbf{x}_{h0} + \mathbf{v}_{h0}\Delta t + \frac{1}{2}\hat{\mathbf{a}}_h \Delta t^2$
3: $\mathbf{v}'_h \leftarrow \mathbf{v}_{h0} + \hat{\mathbf{a}}_h \Delta t$
4: $\mathbf{x}'_r \leftarrow \mathbf{x}_{r0} + \mathbf{v}_r^* \Delta t$
5: $SI \leftarrow -DS\left(\mathbf{x}'_h, \mathbf{v}'_h, \mathbf{x}'_r, \mathbf{v}_r^*\right)$

4.1.1 Algorithm

The purpose of this algorithm is to provide an instant measurement of the human safety given a situation and a robot control input.

The safety index algorithm takes the current human and robot states as input, and is executed at each time step. The algorithm outputs the safety index SI which is a numerical value that represents how dangerous the input states are. The values of SI are real numbers where lower values indicate more danger. Therefore, the lowest value would represent the most dangerous situation, i.e., a collision, while the highest value implies a safe situation. The outline of the algorithm is as follows:

a) Estimate the most dangerous human motion given the human and robot states and the robot control input.

b) Calculate the human and robot states at the time horizon $t + \Delta t$ using the estimated human motion and the robot control input.

c) Calculate a danger score DS assuming a collision between the calculated states.

d) Output the safety index SI as the additive inverse of the danger score DS.

The complete computation at each time step is shown in Algorithm 2, where the input $\mathbf{x}_{h0}$, $\mathbf{v}_{h0}$, and $\mathbf{x}_{r0}$ are the current human and robot positions and velocities, respectively, and $\mathbf{v}_r^*$ is the robot control input. The worst human action

is denoted by $\hat{\mathbf{a}}_h$. The human and robot states at the time horizon $t + \Delta t$ are denoted by $\mathbf{x}'_h$, $\mathbf{v}'_h$, and $\mathbf{x}'_r$, respectively. Note that the human states at the time horizon depend on the worst human action while the robot state depends on the control input. Finally, the safety index is denoted by SI and the danger score by DS.

The human safety algorithm is illustrated in Figure 4.1 using two spheres: human (H) and robot (R). From the initial states (a), the algorithm estimates the worst human action $\hat{\mathbf{a}}_h$ (b). Using $\hat{\mathbf{a}}_h$, the algorithm calculates the human and robot states at $t + \Delta t$ (c). The displacement vector $\mathbf{d}$ between the estimated human position and the robot future position given a control input (d).

4.1.2 Danger Score

In this dissertation, the danger is assessed using the impact severity of a collision between the human and the robot. Actually, this is a collision that would occur if the human takes the worst action, i.e., the most dangerous situation. The collision takes place between an estimated human state and a future robot state, where the danger is rated using a danger score DS.

More specifically, the danger score DS is a function of the human and robot state, defined as follows:

$$DS\left(\mathbf{x}_h, \mathbf{v}_h, \mathbf{x}_r, \mathbf{v}_r\right) = \begin{cases} ds_{\max} & \|\mathbf{d}\| = 0, \\ f_S(\|\mathbf{J}\| \, f_G(\|\mathbf{d}\|)) & \|\mathbf{d}\| > 0, \frac{\pi}{2} < \phi \leq \pi, \\ f_S((1-\rho)\,\|\mathbf{J}\| \, f_G(\|\mathbf{d}\|)) & \|\mathbf{d}\| > 0, 0 \leq \phi \leq \frac{\pi}{2}, \end{cases} \tag{4.1}$$

where $\mathbf{x}_h$, $\mathbf{v}_h$, $\mathbf{x}_r$, and $\mathbf{v}_r$ are the human and robot states, respectively.[10] The impact severity is associated to the impulse $\mathbf{J}$. The displacement vector between human and robot is denoted by $\mathbf{d}$. The functions f_S and f_G are the Sigmoid and Gaussian functions, respectively. The angle ϕ is the angle between $\mathbf{d}$ and the vector of the relative velocity between human and robot. The reliability of the human estimation is denoted by ρ. The maximum value of the danger score is denoted by $ds_{\max}$.

[10]The SI algorithm depends on the human estimation but the danger score does not. Therefore, the input of DS is any human and robot states, whether estimated or current.

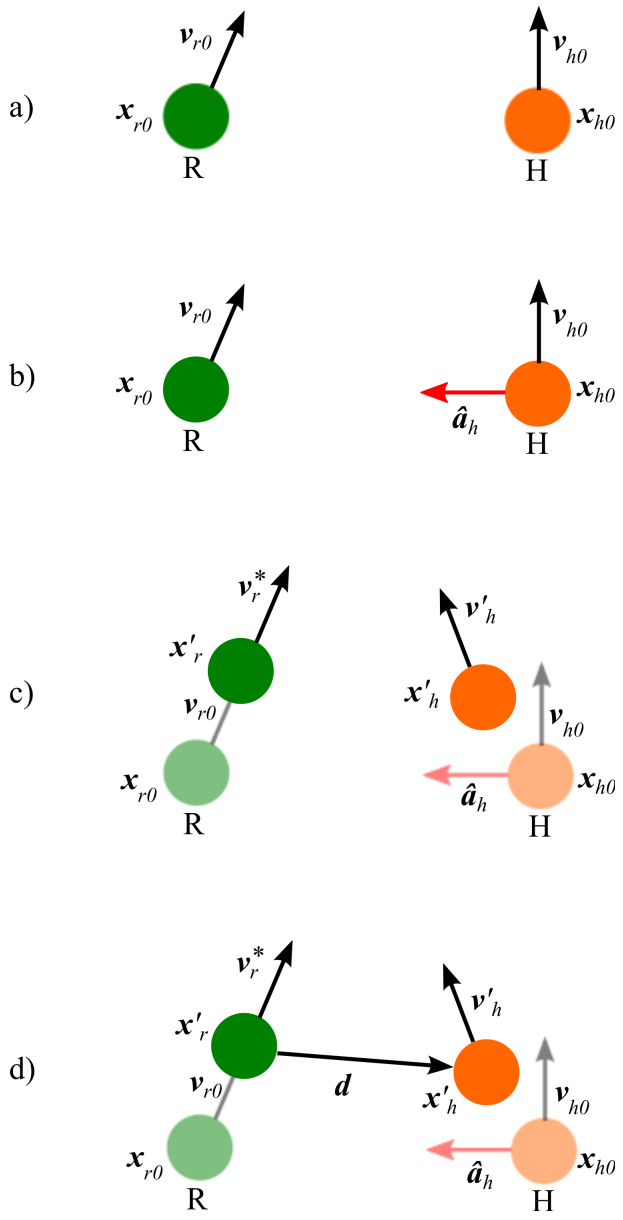

Figure 4.1: Illustration of the Safety Index concept. The initial states of the human (H) and the robot (R) are defined by position and velocity (a). In (b) the worst human action $\hat{\mathbf{a}}_h$ is estimated. Using $\hat{\mathbf{a}}_h$, the algorithm calculates the positions and velocities of the human and the robot at $t + \Delta t$. The displacement vector between the estimated human position and the robot future position given a control input is denoted by $\mathbf{d}$, as shown in (d).

In this dissertation, we define the danger score values as $\mathbb{R} \rightarrow \{2, [0, 1]\}$, i.e., $ds_{\max} = 2$. The details of the danger score formulation are described below.

Impact severity

The impact severity is obtained by calculating the impulse generated during a collision. Impulse $\mathbf{J}$ is defined as the change in the momentum $\mathbf{p}$,

$$\mathbf{J} = \Delta\mathbf{p} = m\mathbf{v}_f - m\mathbf{v}_0, \tag{4.2}$$

where m is the combined mass of human and robot, $\mathbf{v}_f$ if the final velocity, and $\mathbf{v}_0$ is the initial velocity.

Since the initial and final velocities are calculated from the human and robot velocities, Equation 4.2 can be rewritten as:

$$\mathbf{J} = m\left(\mathbf{v}_{h_f} - \mathbf{v}_{r_f}\right) - m\left(\mathbf{v}_{h_0} - \mathbf{v}_{r_0}\right), \tag{4.3}$$

where $\mathbf{v}_{h_0}$, $\mathbf{v}_{h_f}$, $\mathbf{v}_{r_0}$ and $\mathbf{v}_{r_f}$ are the initial and final human and robot velocities, respectively.

Under the assumption that the collision is perfectly inelastic, the final velocities are discarded and we obtain:

$$\mathbf{J} = -m\left(\mathbf{v}_{h0} - \mathbf{v}_{r0}\right), \tag{4.4}$$

where $\mathbf{v}_{h0}$ is the human initial velocity, and $\mathbf{v}_{r0}$ is the robot's initial velocity.

The numerical value of the impact severity corresponds to the impulse norm $\|\mathbf{J}\|$. We normalize this value using a Sigmoid function f_S, as numerical values of DS are easier to interpret if they fall within a known range, namely $\mathbb{R} \rightarrow [0, 1]$. The Sigmoid function f_S has the following form:

$$f_S(x) = \frac{2}{1 + e^{-\beta x}} - 1, \tag{4.5}$$

where β is a parameter to decide how fast the Sigmoid function increases (e.g., if $\beta = 5$ the Sigmoid function increases faster than if $\beta = 1$), and x is the independent variable.

Collisions

To be able to calculate the DS we assume that the human and robot collide. This collision actually does not happen but we use it to calculate the impact severity. There are two key assumptions to support this idea:

a) the human and robot should collide within a finite period of time

b) the collision is perfectly inelastic

With the assumption (a), the states of both human and robot can be calculated, as the time domain is known. The assumption (b) implies that the final velocities of the human and the robot are equal to zero or identical.

We consider three cases, as shown in Figure 4.2:

i) A collision will occur in the worst case.

ii) No collision occurs but the future situation seems to be still dangerous.

iii) No collision occurs and the future situation seems to be safe.

The case (i) reflects situations where the distance between human and robot is zero before the time horizon, which constitutes a very dangerous situation for the human. The discrimination of cases (ii) and (iii) is based on the angle between the relative velocity vector $\mathbf{v}_{\text{rel}}$ and the displacement vector $\mathbf{d}$, derived from their dot product:

$$\phi = \cos^{-1}\left(\frac{\mathbf{d}\cdot\mathbf{v}_{\text{rel}}}{\|\mathbf{d}\|\,\|\mathbf{v}_{\text{rel}}\|}\right), \tag{4.6}$$

where

$$\begin{aligned}\mathbf{v}_{\text{rel}} =& \mathbf{v}_h - \mathbf{v}_r,\\ \mathbf{d} =& \mathbf{x}_h - \mathbf{x}_r.\end{aligned} \tag{4.7}$$

In case (ii), the angle between the relative velocity and displacement vectors is

$$\frac{\pi}{2} < \phi \leq \pi, \tag{4.8}$$

while in case (iii) this angle is

$$0 \leq \phi \leq \frac{\pi}{2}. \tag{4.9}$$

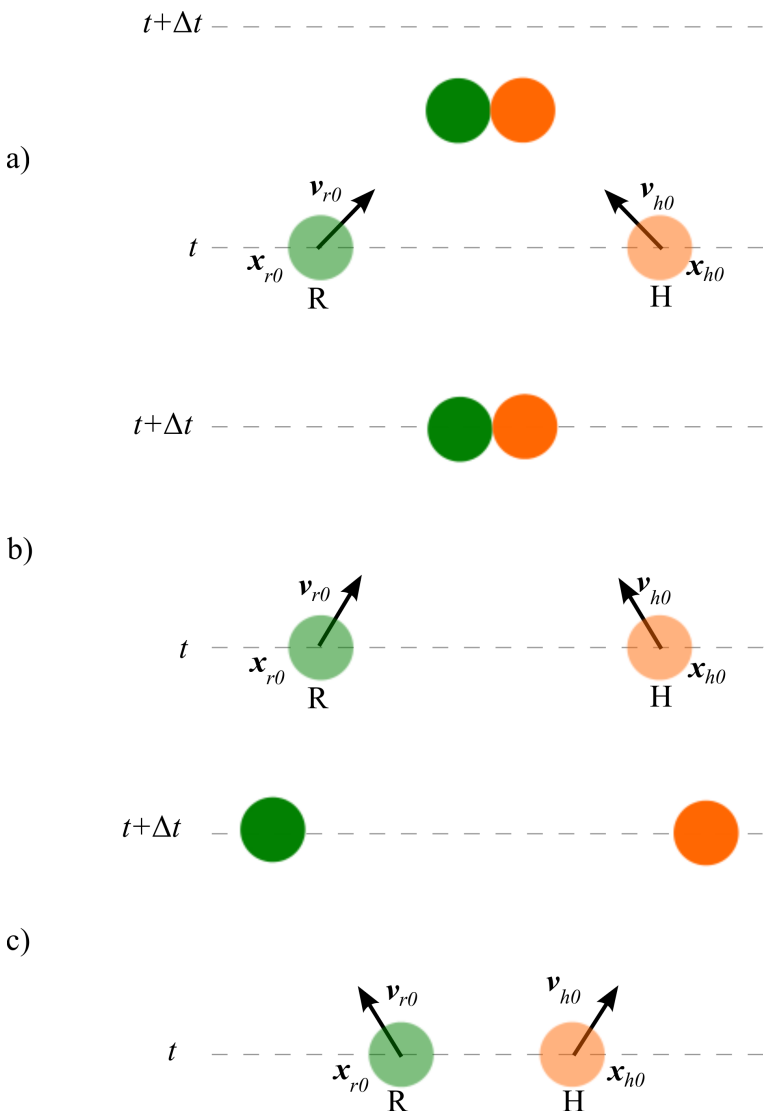

Figure 4.2: Collision cases considered by the safety index algorithm. (a) A collision will occur in the worst case. (b) No collision occurs but the future situation seems to be still dangerous. (c) No collision occurs and the future situation seems to be safe.

A human estimation reliability factor ρ is introduced in the case (iii) to account for the uncertainty of the human motion. This is because we consider less dangerous a situation where a collision is less likely to happen. Nevertheless, the human could erratically change his motion, leading to a danger underestimation. If the reliability is null ($\rho = 0$), the danger around the boundary between cases (ii) and (iii) is similar. In the ideal (but unrealistic) case that the reliability is maximum ($\rho = 1$), the danger in case (iii) can be neglected. In other words, if the human motion is impossible to anticipate ($\rho = 0$), the danger in divergent collisions should be assessed as high as the convergent collision. This opposed to cases in which the human motion is known ($\rho = 1$) and there is no danger whatsoever if the robot is moving away from the human. In this research, a typical value of the reliability is 0.2.

Attenuation by distance

The distance between the human and robot at the moment of the collision is used as an attenuating factor of the danger. This is because a collision far away from the human is less likely to become an actual collision and, therefore, the danger that it represents for the human decreases. On the contrary, a collision when human and robot are very close should be considered as more dangerous since it is more likely to become an actual collision.

The proposed method models the attenuation caused by distance using a Gaussian function f_G.

$$f_G\left(\|\mathbf{d}\|\right) = A \exp\left(-\frac{\left(\|\mathbf{d}\| - B\right)^2}{2C^2}\right), \tag{4.10}$$

where A, B, and C are the parameters of the Gaussian function. In terms of the Gaussian bell shape, the parameter A is the height of the peak, B is the position of the peak's center, and C is the width of the bell.

Asymmetricity

We approach the trade-off between human safety and robot's efficiency using an asymmetric speed restriction.

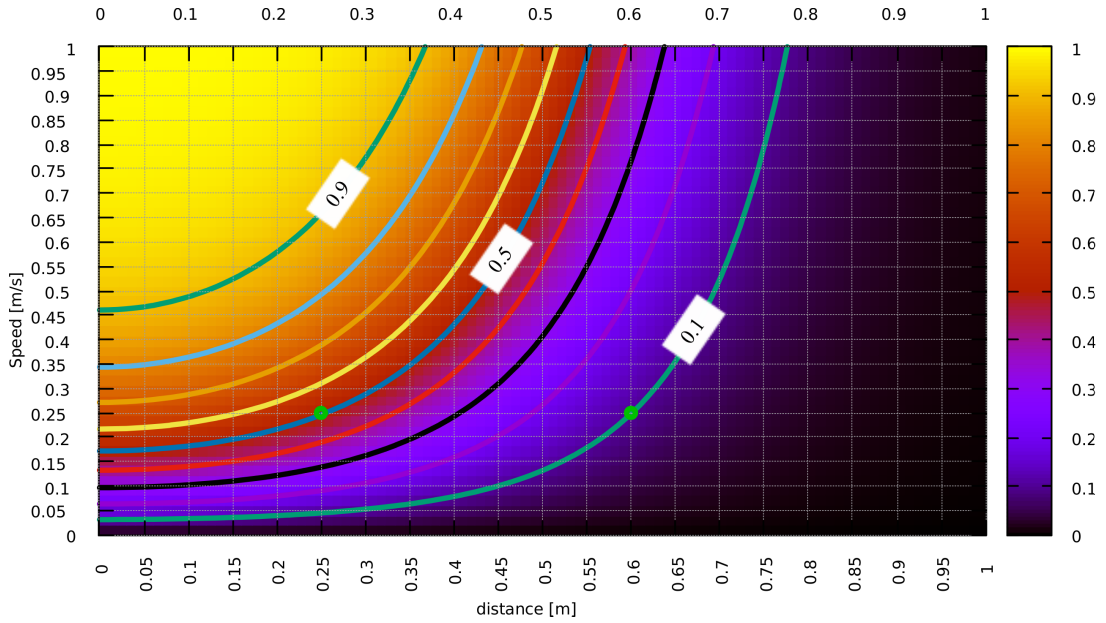

Figure 4.3: Example of the danger relation to speed and distance for case (ii). The danger is 0.1 and 0.5 at 0.6 m and 0.25 m, respectively, when the speed is 0.25 m s^{-1}.

The key to make the safety index asymmetric resides in assigning higher scores to cases where the human and robot are approaching each other (case (ii)) and lower danger scores to the cases where the human and the robot are moving away from each other (case (iii)). To do this, the parameters of the Gaussian and Sigmoid functions are set differently for cases (ii) and (iii). In practical terms, the case (ii) has a wide Gaussian bell and a slowly-increasing Sigmoid function, while the case (iii) has a narrow Gaussian bell and a fast-increasing Sigmoid function.

Figure 4.3 shows an example of the danger relation to speed and distance for case (ii). The small circles highlight the following features of this example. The danger has a value of 0.1 when the distance is 0.6 m and the speed is 0.25 m s^{-1}, while the danger has a value of 0.5 at the same speed when the distance is 0.25 m. Similarly, Figure 4.4 shows an example of the danger relation to speed and distance for case (iii). The danger has a value of 0.1 when the distance is 0.25 m and the speed is 0.25 m s^{-1}, while the danger has a value of 0.5 at the same speed when the distance is 0.1 m. In these graphs we can see that at the same distance the danger increases as the speed increases. By using these graphs,

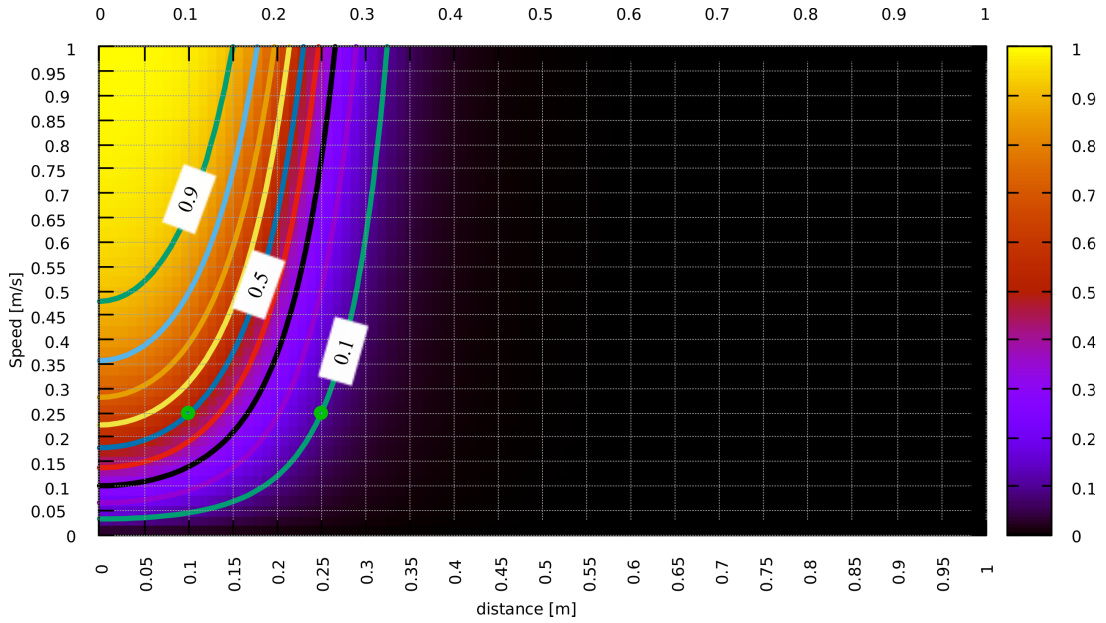

Figure 4.4: Example of the danger relation to speed and distance for case (iii). The danger is 0.1 and 0.5 at 0.25 m and 0.1 m, respectively, when the speed is 0.25 m s^{-1}.

the parameters of the Gaussian and Sigmoid functions can be set for cases (ii) and (iii) according to the safety requirements.

4.1.3 Human behavior modeling

The purpose of modeling the human behavior is to find the human action that results into the most dangerous situation for the human, i.e., the worst human action (WHA). This idea is based on the assumption that if the most dangerous situation is accounted for, the human safety assessment of all other (less dangerous) situations is, consequently, included.

In the proposed scheme, a human action is represented by an acceleration vector. Since this acceleration modifies the human state (position and velocity), it should not produce motions that exceed the physical limits of the human body. We introduce a constant A_h that represents the norm of maximum humanly feasible acceleration.

The estimation of the WHA can be formulated as an optimization problem:

$$\begin{aligned} \underset{\mathbf{a}_h, t}{\text{maximize}} \quad & DS\left(\mathbf{x}_h(\mathbf{a}_h, t), \mathbf{v}_h(\mathbf{a}_h, t), \mathbf{x}_r(t), \mathbf{v}_r^*\right), \\ \text{subject to} \quad & \|\mathbf{a}_h\| \leq A_h, \;\; 0 < t < \Delta t, \end{aligned} \tag{4.11}$$

where $\mathbf{x}_h$ and $\mathbf{v}_h$ are the human states depending on the worst human action and time, and $\mathbf{x}_r$ is the robot position depending on the control input $\mathbf{v}_r^*$ and time. A_h is the maximum human acceleration and the objective function is the danger score DS. As the proposed safety index uses a short-term human behavior estimation, we set a finite period of time Δt (e.g., 400 ms) within which the effects of human actions are predicted. In other words, $\mathbf{a}_h$ is a feasible human action with the highest danger score within the time horizon.

The optimization problem is solved using a Gradient Descent method. To reduce the complexity of this optimization problem, the objective function can be substituted by a function of the distance between the human and robot, namely:

$$F(\mathbf{x}_{h0}, \mathbf{x}_{r0}) = \frac{1}{2} \left\|\mathbf{x}_{h0} - \mathbf{x}_{r0}\right\|^2. \tag{4.12}$$

With this simplification, the optimization problem can be reformulated as:

$$\begin{aligned} \underset{\mathbf{a}_h, t}{\text{minimize}} \quad & F(\mathbf{x}_h(\mathbf{a}_h, t), \mathbf{x}_r(t)), \\ \text{subject to} \quad & \|\mathbf{a}_h\| \leq A_h, \;\; 0 < t < \Delta t. \end{aligned} \tag{4.13}$$

While substituting the objective function reduces the complexity of the optimization problem, the solution becomes suboptimal in terms of DS. Nevertheless, this suboptimal solution can be used as an approximation of the worst human action.

A comparison between the suboptimal solution and a brute force solution is shown in Figure 4.5. This data was obtained by comparing 1000 samples of the danger score DS evaluated using a) a fine-grained brute force method, and b) the proposed solution based on the optimization of $F(\mathbf{x}_h, \mathbf{x}_r)$. The solutions obtained with (a) are used as ground truth. The inferred values obtained with (b) are considered suboptimal in terms of danger. The comparison of these solutions is based on the absolute error. The results indicate an underestimation of danger by the suboptimal solution. Considering that the domain of the danger function DS is $\mathbb{R} \rightarrow \{[0, 1], 2\}$, an absolute error mean of 0.005 ± 0.003 is acceptable.

Algorithm 3: Worst Human Action

Input: $\mathbf{x}_{h0}$, $\mathbf{v}_{h0}$, $\mathbf{x}_{r0}$, $\mathbf{v}_r^*$

Output: $\hat{\mathbf{a}}_h$

1: **for** each $t_i \in [t, t + \Delta t]$ **do**

2: $\quad \mathbf{x}'_{r_i} \leftarrow \mathbf{x}_{r0} + \mathbf{v}_r^* t_i$

3: $\quad$ Find $\mathbf{a}'_{h_i}$ that minimizes F for $\mathbf{x}'_{r_i}$

4: **end for**

5: $\hat{\mathbf{a}}_h \leftarrow \mathbf{a}'_{h_i}$ with minimum F value

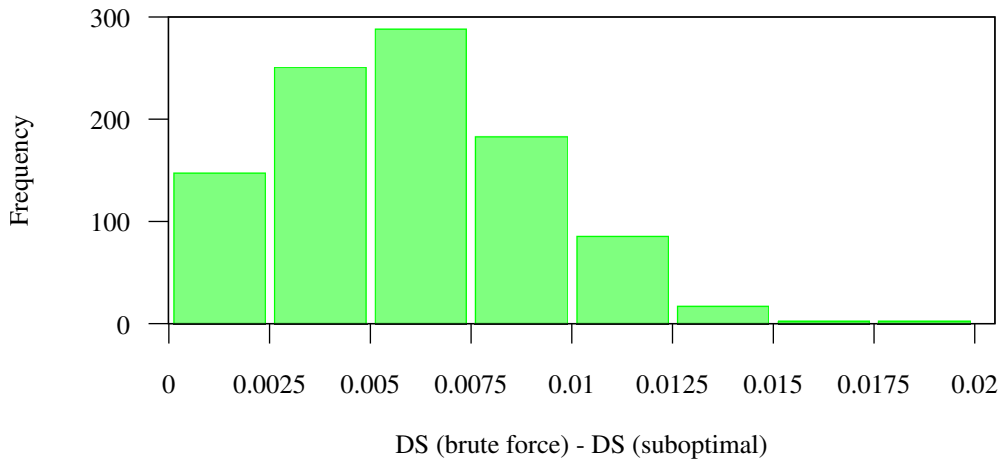

Figure 4.5: Comparison between the suboptimal and brute force solutions of $\hat{\mathbf{a}}_h$ with respect to the danger score. The graph shows that the suboptimal solution underestimates danger within an acceptable error. The error mean is 0.005 ± 0.003.

Algorithm 3 shows the entire computation of the proposed WHA algorithm at each time step. The input is the current human and robot states $\mathbf{x}_{h0}$, $\mathbf{v}_{h0}$, and $\mathbf{x}_{r0}$, respectively. The robot control input is denoted by $\mathbf{v}_r^*$. The output is the worst human action represented by the acceleration vector $\hat{\mathbf{a}}_h$. The time Δt is discretized to make the algorithm practical and is denoted as t_i.

The outline of the algorithm is as follows:

a) Calculate the robot positions $\mathbf{x}'_{r_i}$ for each time sample t_i (step 2).

b) Estimate a worst human action candidate $\mathbf{a}'_{h_i}$ for each robot positions $\mathbf{x}'_{r_i}$ using a Gradient Descent method (step 3).

c) Output the candidate $\mathbf{a}'_{h_i}$ with the minimum value of F as the worst human action (step 5).

Summary

- The analytical approach is based on physical models, in contrast to the heuristic approach based on the human notion of danger.
- SI is an instantaneous measurement of human safety given the human and robot states and a robot control input.
- We model the human behavior to maximize the danger in order to know the borderline of danger in the given situation.
- SI numerically represents the human safety by calculating the severity of a collision between an estimated human state (from the human behavior model) and a future robot state (from the control input).

4.2. Generalized Velocity Moderation

In this section, Generalized Velocity Moderation (GVM) which is a controller that adjusts the robot's velocity to keep human safety is proposed. To guarantee human safety, we consider the relationship between the whole bodies of the human and robot. Depending on such relationship, we restrict the robot speed under the assumption that the lower the speed, the safer the robot motion is.

The proposed controller is capable of interchangeably using different human safety metrics. The need for a controller that can quickly adapt the safety of the robot's motion to new scenarios is patent, as human safety requirements vary depending on the application. Moreover, the continuous release of safety standards[11], triggers the necessity of modifying or replacing currently used human safety metrics.

As opposed to a simple modification of the parameters of the human safety metric, the proposed controller can switch the human safety metric itself. This is because there is an inherent limitation when only modifying the parameters to meet the human safety requirements of the intended application, as the core of the human safety metric remains unchanged. In this sense, the proposed method is a flexible controller designed to use different human safety metrics in an interchangeable manner.

The proposed controller is applicable to tasks whose velocity is not critical, such as pick-and-place. For tasks that depend on specific velocities, such as catching a ball, a higher-level planner is necessary.

To test the proposed controller, we perform real-robot and simulation experiments where the human and robot do simple tasks in shared workspaces. The experimental results validate the proposed method as a flexible controller independent of the human safety metric.

This section is organized as follows. Section 4.2.1 is an overview of the GVM controller. Section 4.2.2 contains the details of the algorithm. Section 4.2.3 explains the usage of GVM with a human safety metric. Section 4.2.4 describes the balance between human safety and the robot's efficiency.

[11]The technical specification TS 15066 [17] for power and force limited collaborative robots is supposed to be released in the coming months.

4.2.1 Overview

GVM is a low-level controller to guarantee human safety. Keeping human safety is achieved by restricting the robot speed. The core idea of GVM is to consider both human safety and the robot's performance by allowing the robot to move as fast as possible without violating a human safety constraint.

The input of GVM is a trajectory of joint angles. The output of GVM is the target joint angles used to follow the trajectory in an on-line manner, where speed is restricted to ensure human safety. The speed is restricted by temporarily remapping the points on the trajectory without modifying the original shape of the motion, which we assume does not affect the task completeness.

In GVM, we consider representative points on the robot and on the human, such as joints. We estimate the human safety for every combination of the representative points using a human safety metric (HSM). The human safety evaluation (HSE) of the most dangerous combination is used as the overall safety. Then, GVM restricts the robot speed until a human safety constraint is satisfied. Finally, the resulting restriction is used for the actual temporal-remapping.

4.2.2 Algorithm

The GVM algorithm takes a time-parametrized trajectory $\mathbf{q}(t)|t \in [0, T_{\text{end}}]$ as input, and is executed at each time step Δt until $\mathbf{q}(t)$ is completed. GVM outputs the target joint angles $\mathbf{q}^*$ at each Δt according to the speed restriction. The temporal remapping is done by calculating a *trajectory scaler* $s \in [0, 1]$ that indicates the degree of velocity modification; when $s = 1$ the robot will move at the original speed, and when $s = 0$ the robot will stop. An *internal time* $\tilde{t}$ is tracked to preserve the trajectory shape. GVM starts with $\tilde{t} = 0$. At each Δt, $\tilde{t}$ is incremented by $s\Delta t$.

For every combination of points on the robot $j \in \{1, \ldots, m\}$ and points on the human $h \in \{1, \ldots, n\}$, a human safety evaluation hse_{jh} is computed using the human safety metric function f_{HSM}. This computation depends on the points' state $\mathbf{x}_{jh}$, as well as on the control input $\mathbf{u}$ to modify the robot's state from $\mathbf{q}_{\text{curr}}$ to $\mathbf{q}(\tilde{t}+s\Delta t)$, e.g., velocity. If the safety constraint ζ_{HSM} is violated, the scaler s is decreased by a constant k (e.g., 0.05). This is repeated until the safety constraint

Algorithm 4: Generalized Velocity Moderation

Input: Δt, $\tilde{t}$, $\mathbf{q}(t)|t \in [0, T_{\text{end}}]$, $\mathbf{q}_{\text{curr}}$, $\{\mathbf{x}_{jh}|j \in \{1,\ldots,m\},\ h \in \{1,\ldots,n\}\}$ f_{HSM}, ζ_{HSM}

Output: $\mathbf{q}^*$, $\tilde{t}$

$s \leftarrow 1$
while $s > 0$ **do**
  $\mathbf{u} \leftarrow F\left(\mathbf{q}(\tilde{t} + s\Delta t) - \mathbf{q}_{\text{curr}}\right)$
  for each robot point j **do**
    for each human point h **do**
      $hse_{jh} \leftarrow f_{\text{HSM}}(\mathbf{x}_{jh}, \mathbf{u})$
    end for
  end for
  $\hat{hse} \leftarrow \min\left(hse_{jh}\right)$
  if $\hat{hse} < \zeta_{\text{HSM}}$ **then**
    $s \leftarrow s - k$
  else
    break
  end if
end while
$\mathbf{q}^* \leftarrow \mathbf{q}(\tilde{t} + s\Delta t)$
$\tilde{t} \leftarrow \tilde{t} + s\Delta t$

is satisfied or $s = 0$. Finally, the controller outputs the target joint angles which comply with the safety constraint.

Algorithm 4 shows the entire computation at each time step. The current joint angles are denoted by $\mathbf{q}_{\text{curr}}$.

The GVM algorithm does not depend on the selection of representative points, so this selection can be changed according to the situation. In this work, GVM computes the human safety evaluation for every combination of a point j on the robot's joints and a point h on the human joints. We consider these representative points as reasonable for articulated robots such as humanoid robots.

4.2.3 Usage with a human safety metric

To be able to use a human safety metric with GVM, it is necessary that:

- the domain of the human safety metric function f_{HSM} is known
- a safety constraint ζ_{HSM} is provided

The GVM controller maintains the human safety of the interaction compliant with the safety constraint. Even though the domain of f_{HSM} is easier to interpret if it is finite, a domain with one or both extremes set to infinity can be used. In the absence of the safety constraint, the controller is unable to guarantee human safety since this is the only clue it has about how the human safety metric assess safety and the intended human safety *level*. If the constraint is set to infinity, the controller will not allow the robot to move or allow non-restricted motion, depending on the human safety metric design.

4.2.4 Safety and efficiency balance

The safety constraint can prioritize human safety over robot's efficiency, and vice versa. GVM ensures human safety by modifying the robot's speed to comply with a safety constraint. To reduce the impact on the robot's performance caused by the human safety enforcement, GVM aims to move the robot as fast as possible within the limits of that safety constraint. Therefore, making the safety constraint stricter results in a safer HRI but also in a diminished robot's efficiency. On the other hand, relaxing the safety constraint allows the robot to move at higher

speeds in a closer proximity to the human. This benefits the robot's efficiency but reduces the available time to react to human motions and the tolerance to the uncertainty of those motions, which may compromise human safety.

GVM is not asymmetric *per se* but depends on the human safety metric being asymmetric. The GVM nature of a flexible controller for human safety requires an independence from the human safety metric. The lack of intrinsic asymmetricity allows GVM to accommodate a broader range of human safety metrics, both symmetric and asymmetric.

Summary

- GVM is a controller capable of using different human safety metrics.
- GVM maintains human safety by modifying the robot speed to comply with the safety requirements.
- The robot's performance is maintained by moving the robot as fast as possible without violating the safety requirements.
- GVM is a general framework that others researchers can use to test their safety metrics or new standards.

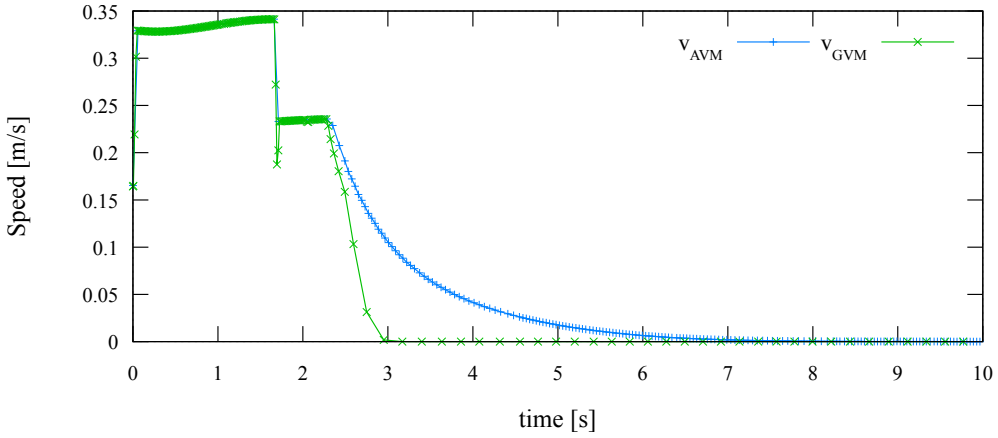

Figure 4.6: Speed profiles of AVM and GVM-SI. The speed profiles are as similar as possible to achieve a fair comparison.

4.3. Experimental results

In this section, GVM using the Safety Index, or GVM-SI, is compared to AVM in terms of a) human safety by simulating a dangerous situation, and b) efficiency using eight simplified HRI scenarios, both with simulation experiments. The experimental setup is the one described in Section 3.3.

In order to compare GVM-SI to AVM, a common ground should be established. Therefore, a fair comparison criteria is introduced in this section. Moreover, the asymmetric property of GVM-SI is tested using a moving-toward and moving-away motion. A comparison in terms of human safety is carried out using a simple motion where human and robot move toward a collision. Finally, the robot's efficiency is evaluated by measuring the task completion time in eight simplified HRI scenarios.

4.3.1 Fair comparison

AVM and GVM-SI are intrinsically different. Beyond the theoretical difference of their approaches, there is a parametric difference. While AVM requires two distance thresholds and a maximum allowed velocity to be set, GVM-SI requires the Sigmoid and Gaussian parameters, and the safety constraint to be set. The

difference in the parameters' nature poses a challenge to fairly compare these methods as an arbitrary configuration would make one method safer or more efficient than the other.

To fairly compare AVM and GVM-SI in terms of human safety, we modify the parameters of GVM-SI to behave as similar as possible to the AVM configuration used in Section 3.4. The criteria to make them similar is to start the restriction of the robot speed at the same time. Then, reduce the robot speed with similar profiles. We use a simple robot motion in proximity of a motionless human in order to make AVM and GVM-SI have similar speed profiles. As SI considers the human velocity, making the human stand still eliminates such advantage, which allows a fair comparison of these methods.

The Sigmoid and Gaussian parameters of GVM-SI are modified until the robot is able to complete a simple motion in a similar way to AVM, as shown in Figure 4.7. The similarity between the speed profiles of AVM and GVM-SI is shown in Figure 4.6. The profiles correspond to the speed of the robot's end-effector.

The robot speed is the same with both methods until the time where the restriction starts. With AVM, the speed reduction is smooth until the robot comes to a complete stop. The speed decreases faster in the case of GVM-SI. This is because, in spite of the human standing still, SI estimates a human state with a non-zero speed. As GVM-SI estimates the danger of a collision with that state, it makes the speed drop faster than AVM. Moreover, the estimated human state is closer than the actual human is. GVM-SI uses the distance to the estimated human position while AVM uses the distance to the actual human position. This difference causes a higher speed restriction by GVM-SI.

4.3.2 Asymmetricity

The purpose of this experiment is to demonstrate the asymmetric property of GVM-SI, as the trade-off between human safety and efficiency is approached with an asymmetric restriction.

With a human standing still, the robot moves toward the human until its speed is almost zero. Then, the robot moves away from the human using the same motion in the opposite direction. The speed profile of the robot's end-

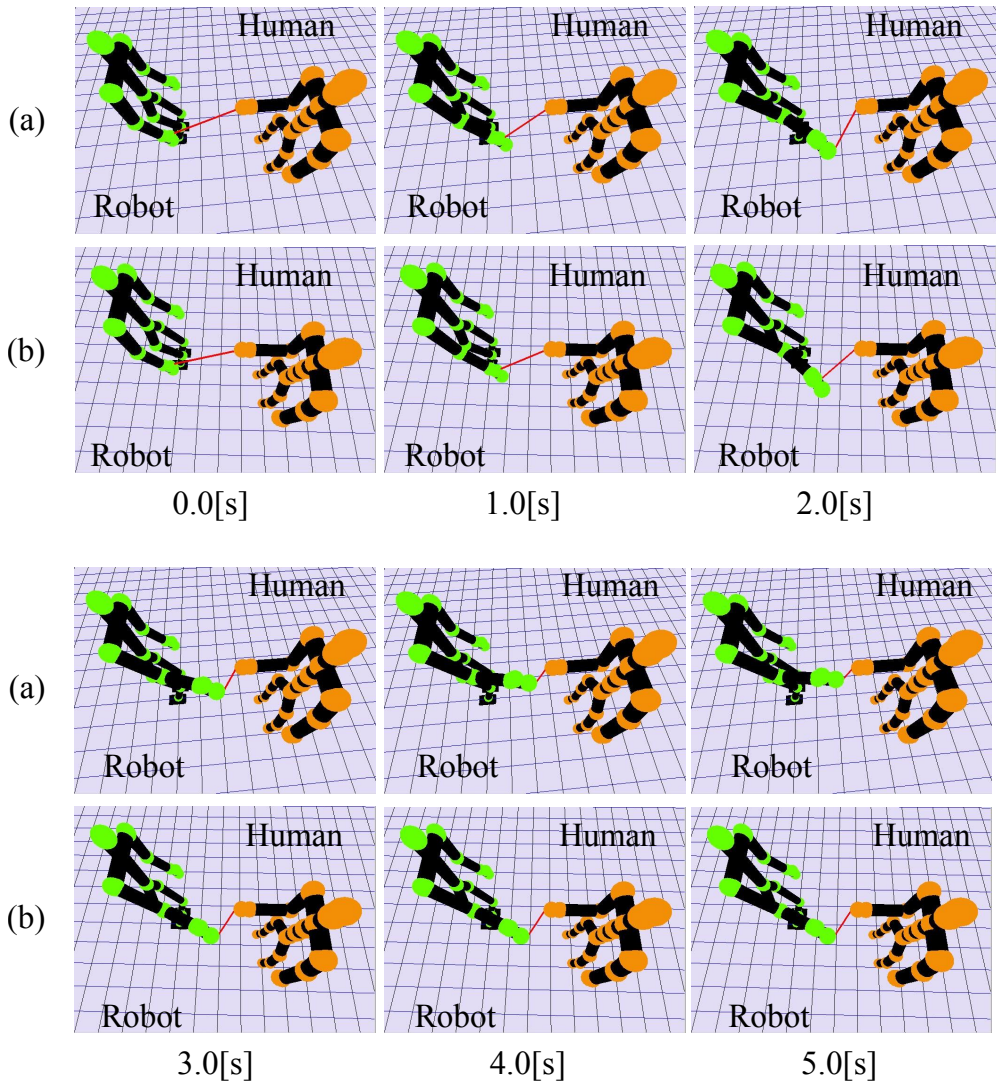

Figure 4.7: Screenshots of the fair comparison between AVM (a) and GVM-SI (b) using a motionless human. Here, both methods make the robot to perform a simple motion a similar manner.

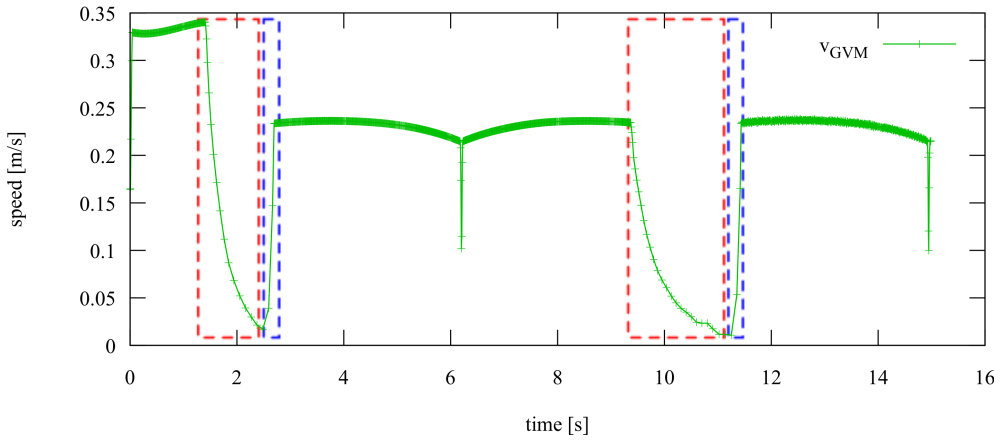

Figure 4.8: Asymmetricity of GVM-SI. Regions in red represent the approaching motions while the blue regions represent the moving away motions. The red regions wider than the blue regions indicate that the asymmetric speed restriction is achieved.

effector is shown in Figure 4.8. The regions highlighted in red correspond to the approach motions, while the regions highlighted in blue correspond to the moving away motions. The difference between the restriction of approaching and moving away motions confirm that the asymmetric property of GVM-SI is achieved.

The Figure 4.9 shows the screenshots of the experiment from time 9.33 s to 13.33 s. The row (a) corresponds to the approaching motion while row (c) corresponds to the moving away motion. The frame in (b) is the time where human and robot are closest and the robot speed is almost zero.

4.3.3 Human safety comparison

In these experiments, we compare the robot's response to the incoming collision with the human hand using the proposed safety index and AVM, as shown in Figure 4.10. We compare the speed profiles of these methods using the same human motion and the same robot's trajectory.

We add two test cases to verify the proposed safety index. We consider that these test cases are dangerous situations that humans may face in daily-life scenarios.

TC-5. The human and the robot are moving their hands toward a direct collision.

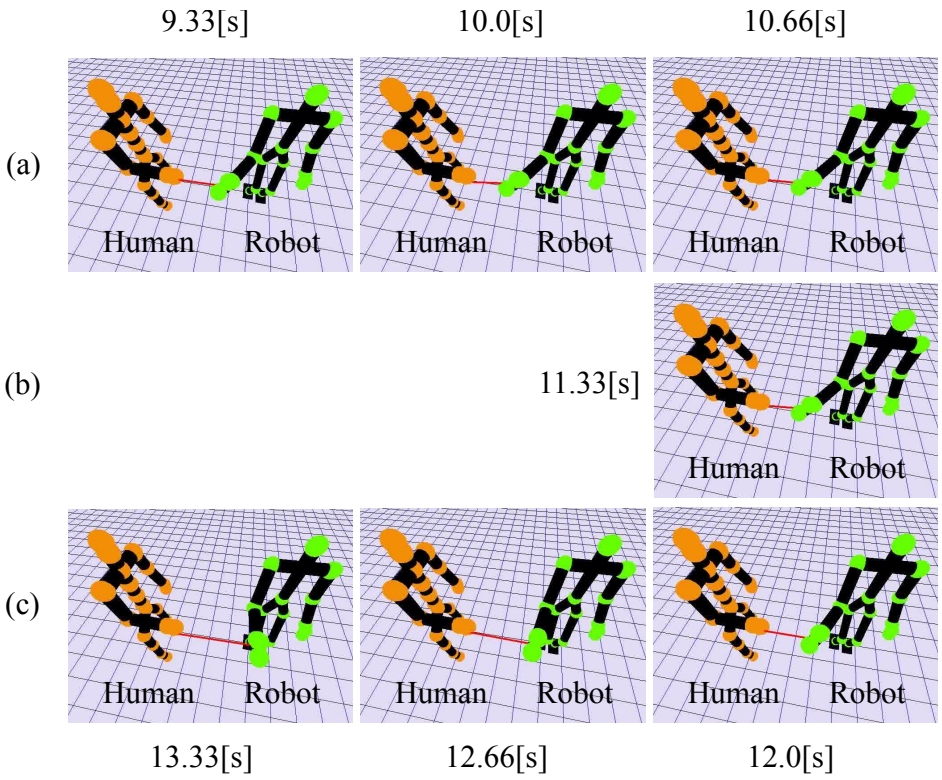

Figure 4.9: Screenshots of the asymmetricity test of GVM-SI. Row (a) corresponds to the approaching motion. The frame in (b) corresponds to the time where the human and the robot are closest and the robot speed is almost zero. Row (c) corresponds to the moving away motion.

In this dangerous situation, the velocity vectors are parallel.

TC-6. The human and the robot are moving their hands toward a common region. In this dangerous situation, the velocity vectors are perpendicular.

In TC-5, the robot starts to restrict the robot speed earlier than AVM, as shown in Figure 4.11(a). This is because the safety index is estimating the WHA which consists of increasing the velocity of the human end-effector toward the robot's end-effector. The impact severity of such estimated velocity contributes to increase the danger score. Moreover, the estimated human position is closer than the actual human which also increases the danger score.

Similarly in TC-6, the robot speed restriction starts earlier than AVM, as shown in Figure 4.11(b). In this case, the WHA consists of increasing the velocity

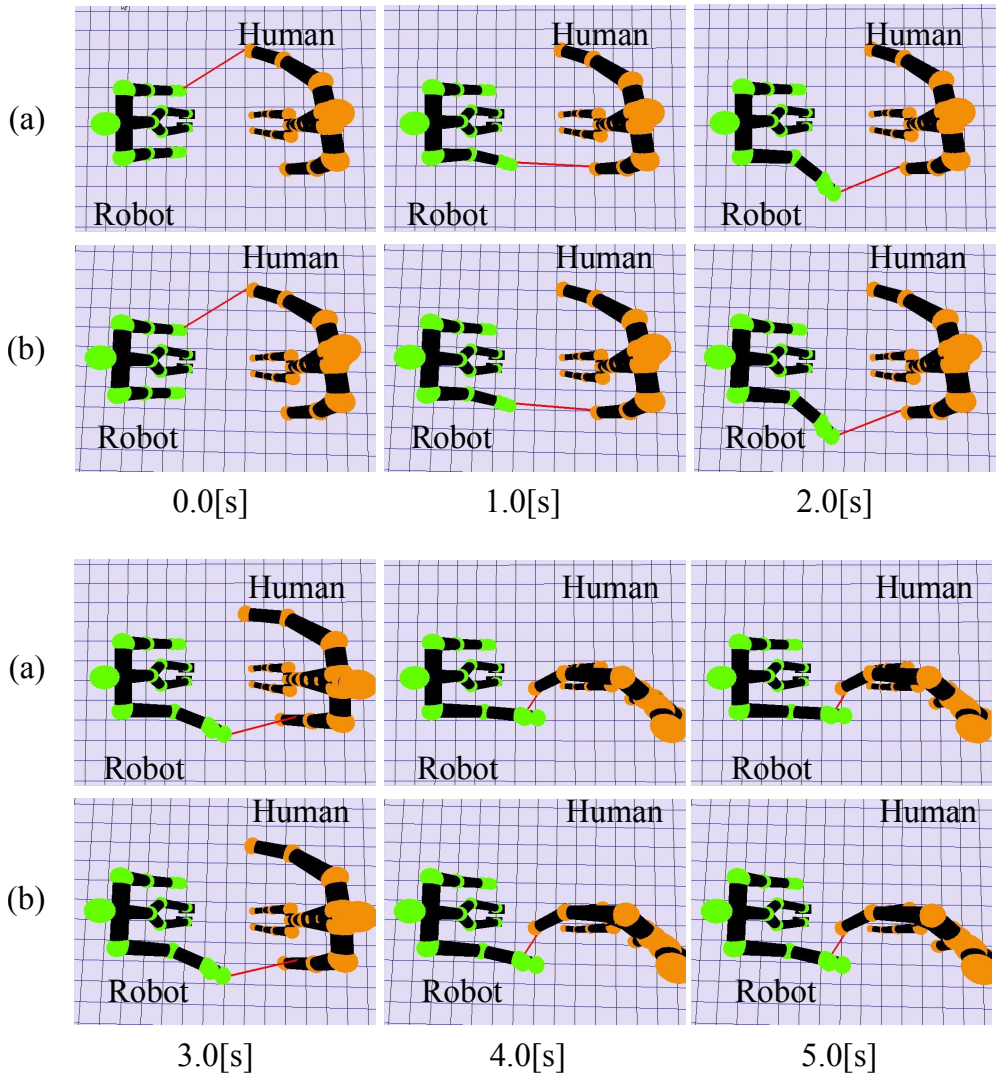

Figure 4.10: Screenshots of the test case to compare human safety between AVM (a) and GVM-SI (b) using a motion where human and robot move their hands toward each other. Here, GVM-SI makes the robot stop earlier than AVM.

toward the point where the trajectories of the human and robot end-effectors intersect. The increase in the velocity contributes to a higher danger score. The estimated human position in the vicinity of the trajectories' intersection also contributes to increase the danger score.

Figure 4.12 shows the speed profiles of the human and robot's end-effectors for TC-5. Before the human moves, the robot speed with both methods is the same. With the proposed safety index, the robot speed is restricted earlier than with AVM, approximately 200 ms before. This translates into an increase of distance for reaction to the human motions, e.g., if the relative velocity is 0.8 m s^{-1}, the restriction of GVM-SI would occur 0.16 m before AVM. In other words, the safety index is more cautious when approaching the human in anticipation of a collision.

To compare the speed restrictions, we calculated the restrictions that GVM-SI and AVM would output but without actually controlling the robot motion. A similar test case is used, the only difference is that the robot speed restriction is not applied but only calculated. In other words, the robot traverses the trajectory without restricting its speed. This was necessary because of the obvious delay that any of the methods would introduced if they were modifying the robot speed.

The resulting speed restrictions are shown in Figure 4.13. In the case of GVM-SI, the speed restriction occurs earlier than AVM (around 0.4 s before). As the robot is not modifying the speed, the speed restriction of both methods quickly becomes strict during the approach motion. On the other hand, AVM relaxes the restriction earlier than GVM-SI as the human and the robot start to move away[12]. As GVM-SI considers an estimated human state that is closer and moves faster than the actual human does, the speed restriction is stricter.

4.3.4 Efficiency evaluation

Simulation experiments are carried out to compare the efficiency of AVM and GVM-SI. In these experiments, the parameters of the fair comparison are used. The tested HRI scenarios are described in Section 3.3.

The experiments consist of executing each method 10 times for each setup. As detailed in Section 3.3, the human task is to move objects above a table and

[12]The restriction by AVM around $t = 6$ s is caused by another joint (not the end-effector) toward which the robot is moving

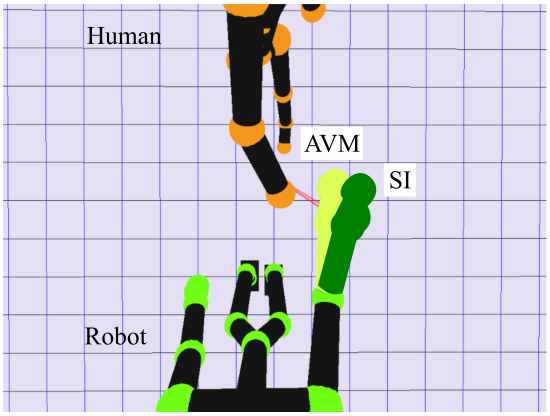

(a) TC-5

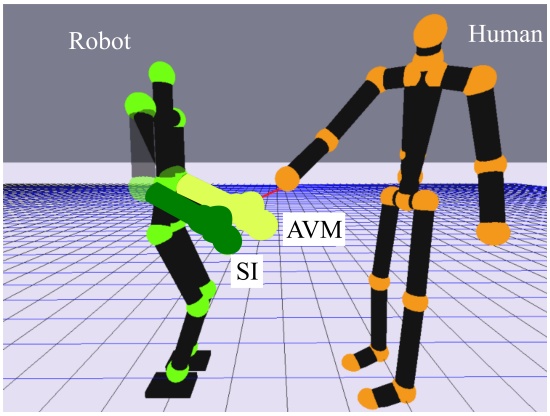

(b) TC-6

Figure 4.11: Simulation experiments with the test cases for the human safety comparison. The superposition of the robot states shows the configuration where the robot stops with each method. The clear color corresponds to AVM while the dark color corresponds to SI.

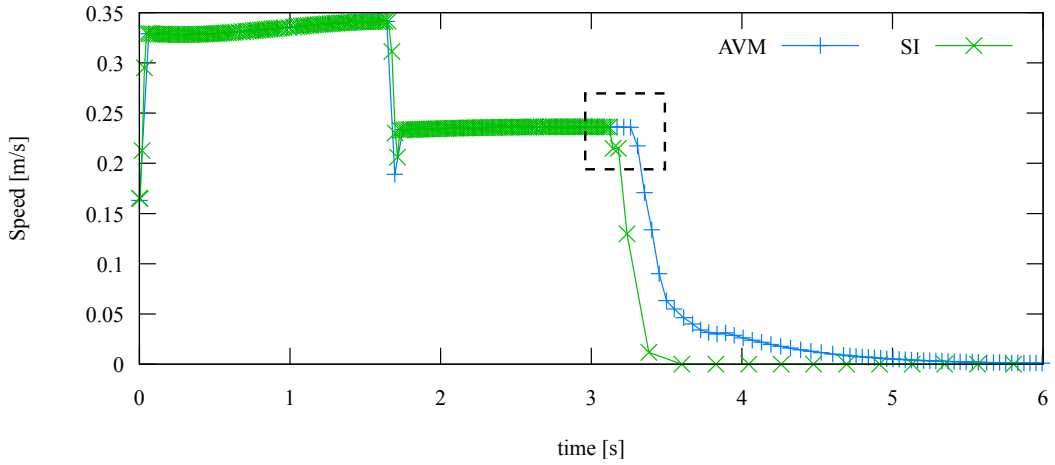

Figure 4.12: Speed profiles of SI and AVM for the test case TC-5. The speed profiles show an earlier stop of GVM-SI which demonstrates the advantage of the human behavior estimation.

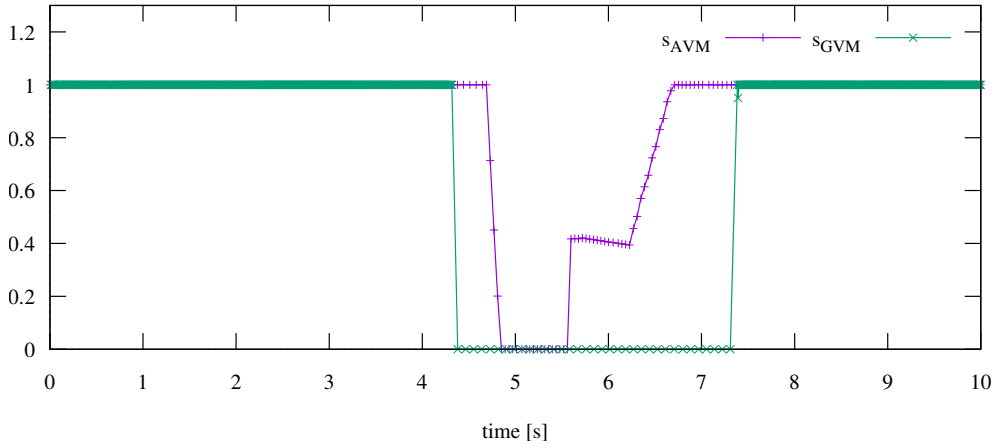

Figure 4.13: Scalers of AVM and GVM-SI for the test case where the robot speed is not restricted.

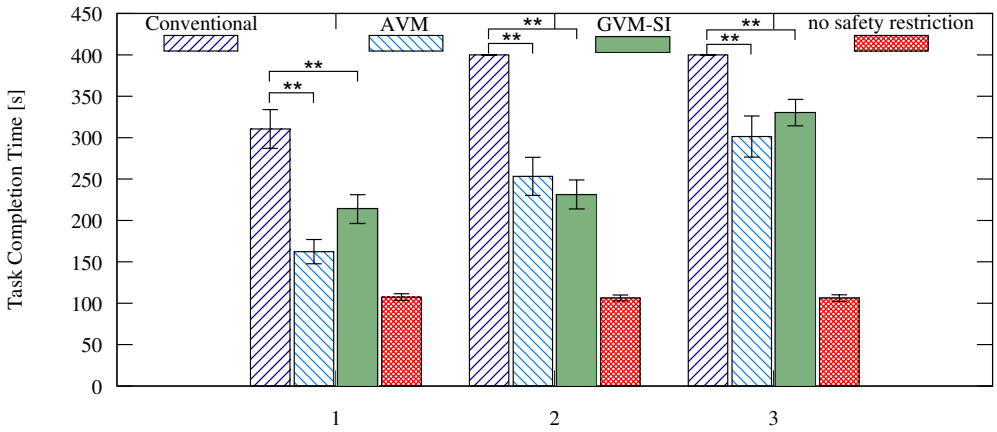

Figure 4.14: Task completion time of GVM-SI with fair comparison parameters and the safety constraint ζ_{SI} set to -0.8. Lower time indicates better robot's performance. Setups 1 and 6 show the expected delay in GVM-SI caused by the earlier restriction. In setup 2, GVM-SI shows a better performance but not significantly.

the robot task is to randomly place the end-effector to preset positions above the table. The safety constraint ζ_{SI} is set to -0.8.

As GVM-SI anticipates the human motion, the speed restriction occurs earlier than AVM. In setups 1 and 6, the delay caused by this earlier restriction is patent, as shown in Figure 4.14. In setup 2, GVM-SI shows a better performance but not significantly.

In all setups, GVM-SI shows a better performance than the conventional method. GVM-SI is outperformed by AVM but it is still competitive.

Summary

- AVM and GVM-SI are fairly compared using a criteria where both methods behave similarly in specific conditions.
- The asymmetric property of SI is verified to ensure the robot's performance is maintained.
- We present a detailed analysis of human safety using two test cases where the human and robot move their hands toward a collision.
- GVM-SI reduces the robot speed earlier than AVM as GVM-SI estimates the human motion.
- The robot's efficiency is evaluated by measuring the task completion time in three HRI scenarios.
- GVM-SI overcomes the conventional method and has a competitive performance.

4.4. Discussion

In this section, we discuss when AVM should be used instead of GVM-SI and vice versa.

4.4.1 Comparison between AVM and SI

A debatable question rises when comparing AVM to SI: which one is safer?

SI is theoretically better supported than AVM as SI physically measures the severity of a collision while AVM implements the human notion of danger directly into the robot control. Moreover, SI estimates a human action whose danger cannot be theoretically exceeded by any other human action. This makes SI better reflect the actual human safety state, as it is considering the danger borderline (i.e., a threshold beyond which there are no more dangerous situations).

We can differentiate between an ideal SI which is purely based on physical models and a practical implementation of SI where some assumptions are made (such as the one implemented in this dissertation). The ideal SI should be better than AVM as it is exempt from danger underestimation issues. On the other hand, the practical SI may be better than AVM if the consequences of the assumptions of SI overcome the consequences of the danger underestimations of AVM.

The answer to the raised question can just be answered to the extent of the nonexistent human safety ground truth: we consider that SI may be redundantly safer than AVM in some cases, while AVM may be violating human safety in some other cases.

4.4.2 Applicability

Apart from the parametric difference of AVM and GVM-SI, the different computational cost and the preferable applicability of one controller over the other for certain tasks or scenarios are debatable.

Regarding the computational cost, GVM-SI has a relatively high cost caused mainly by the estimation of the worst human action and the time discretization, while AVM has a relatively low cost. In applications demanding the human safety estimation over a large number of representative points (e.g., one robot

and multiple humans), the computational cost may become forbidding. In such cases, AVM is a more affordable solution.

There are some possible modifications at the implementation level that can be done to reduce the computational cost. For example:

1. Optimize the scaler calculation to avoid iteratively decreasing the scaler value until it satisfies the safety constraint.
2. Use a Gradient Descent method that converges faster such as ADADELTA proposed by Zeiler [46].
3. Calculate the SI only for moving joints.
4. In the particular experiments proposed in this dissertation, the calculation of SI for the human legs can be skipped.

Besides the computational cost, factors such as the variability of the task, the familiarity of the robot to the human, and the ratio of unexpected/expected human motions should be considered for the selection of the controllers. GVM-SI is more cautious when interacting with the human due to the estimation of the worst human action of the Safety Index than AVM which is purely reactive. Then, GVM-SI is better suited for tasks with high variability (i.e., the robot requires multiple motion primitives) such as assembling, while AVM is better suited for tasks with low variability such as pick-and-place. Moreover, GVM-SI is better suited for scenarios where the human is not familiar with the robot (e.g., service robots in public places) while AVM can be used at home or in a factory where humans are familiar with the robots using the proposed controllers. Furthermore, GVM-SI is better suited for interactions with high number of unexpected human motions. As humans perform the same task in different ways and some humans are more consistent in their motions than others, a more cautious controller is more suitable.

Summary

- In this chapter, we presented two methodologies as part of our analytical approach to human safety: SI and GVM.
- SI is an instantaneous measurement of human safety which considers the potential injuries and the most dangerous situation.
- The numerical value of SI represents the severity of a collision and the probability of that collision to occur.
- GVM is a general framework that maintains human safety according to the input human safety metric and the human safety requirements.

Chapter 5

Conclusions

In this chapter, the conclusions of this dissertation are presented, as well as the particular conclusions for each approach.

5.1. General

The proposed methods presented in this dissertation conform solutions to the human safety problem which stipulates that the risk of injuring the human should be kept under acceptable limits while complying with performance requirements.

In particular, methods to quantitatively assess human safety and controllers to make the robot use only human-safe motions while being efficient are proposed.

5.1.1 Assessment

This dissertation used 1) the distance and direction of motion and 2) the severity of potential human injuries to assess human safety. Both metrics provide a numerical representation of the human safety status given a state and a control input. While (1) was effectively used to guarantee human safety, it lacks the connection to the actual damage a robot action could cause in the human body, which is achieved by (2).

In this dissertation, human behavior estimation is integrated to the human safety assessment. The proposed estimation consists of finding the human action

that maximizes the danger, which provides the danger borderline whose limits the robot should not violate. The proposed human behavior estimation resulted in an earlier restriction of the robot motion, which allows bigger time and distance margins to guarantee human safety.

A whole-body relationship through representative points located on both human and robot bodies is used in this dissertation. Human safety is independently assessed for every possible combination of the representative points. Finally, the human safety assessment of the most dangerous combination is used to represent the human safety of the whole-body relationship.

This dissertation studied the asymmetric property of the robot motion restriction which benefits the efficiency of the robot without sacrificing human safety. The proposed methods give higher safety scores to cases where the human and robot are moving away from each other and lower safety scores to cases where the human and robot are moving toward each other. This leads to a more cautious robot behavior when approaching the human and to a more efficient robot behavior when moving away from the human.

5.1.2 Control

In this dissertation, the controllers operate under the assumption that the lower the speed the safer the robot motions are for the human. Therefore, a trajectory scaling technique to modify only the speed of the input trajectory while preserving its shape was implemented. This allows the robot to keep moving even at lower speeds as long a human safety constraint is satisfied.

As there are avoidable collisions, there are others which cannot be avoided. The proposed controllers are designed to ensure that the robot comes to a complete stop before a collision occurs. If such collision occurs, it can be inferred as a collision caused by the human.

This dissertation proposed two controller schemes: safety metric dependent and independent. The benefit of the independent scheme resides in its capacity to interchangeably use multiple safety metrics without altering the controller itself. Such scheme requires an explicit safety threshold under which the controller should keep the robot motions, which is the only notion of the controller about what safe and dangerous is.

5.2. Heuristic approach

This dissertation proposed Asymmetric Velocity Moderation as a low-level controller to ensure human safety and performed real-robot and simulation experiments involving human subjects and a humanoid robot. The obtained results include a detailed comparison of human safety in dangerous situations. Moreover, the task completion time to evaluate the robot's efficiency in simplified HRI scenarios is reported.

AVM considers the distance and also the direction of the motion to determine whether to limit the robot's speed. The proposed method restricts the robot motion more when it is moving toward the human and relaxes the restriction when the robot is moving away from the human. With AVM, a robot can deal with simplified HRI scenarios and perform tasks using only human-safe motions. Moreover, when used as a low-level controller along with behavior-specific strategies, AVM can audit the robot motion and ensure it is human-safe.

The proposed method better assesses the risk of a collision when approaching the human and decreases the speed of the robot both smoothly and earlier, in comparison to conventional and non-asymmetric methods. In spite of the sacrifice in efficiency, the proposed method is still competitive and significantly faster than the conventional approach.

The heuristic nature of AVM makes it an easily-implementable and widely-applicable controller for human safety.

5.3. Analytical approach

In this dissertation, a safety index as a human safety metric which estimates the human behavior to anticipate dangerous situations is proposed. Moreover, Generalized Velocity Moderation is proposed as a controller for human safety which can accommodate different human safety metrics in an interchangeable manner. Simulation experiments involving a human and a humanoid robot were carried out. Additionally, the robot's efficiency in simplified HRI scenarios was evaluated in terms of the task completion time.

The proposed safety index estimates the worst possible human action to de-

termine the safety of the interaction. By considering the worst human action, the proposed method provides a numerical evaluation of the most dangerous situation. Human safety assessment is related to the injuries that the robot could inflict to the human if a collision occurred when the human takes the worst possible action. The experiments results show an earlier restriction and a cautious robot behavior as it effectively estimates the human behavior anticipating the most dangerous situation.

The proposed controller keeps human safety by restricting the robot speed to satisfy a safety constraint. To keep a good performance, the controller allows the fastest robot speed that satisfies the safety constraint. By modifying the safety constraint, the trade-off between human safety and efficiency can be adapted to the requirements of the application. The experiments results show that the controller keeps human safety while achieving competitive task completion times.

5.4. Future work

Situations where the robot uses tools or transports objects are of special interest since we can find multiple examples in daily-life environments (e.g., the robot transports a box or the robot uses a screwdriver). The methods proposed in this dissertation can be modified to include these cases by extending the representative points to cover the surface of the transported objects. This would provide human safety as long as the object a) is passively safe (e.g., the object is not hot or sharp) and b) remains under the manipulation of the robot (i.e., it is relatively fixed to a robot link or the end-effector). When the condition (a) is not present, virtually expanding the size of the objects can be a reasonable solution to maintain safety. As condition (b) can be accidentally broken when transporting the object (e.g., a collision with the environment or a slippery object), the potential energy of the object should be considered. A practical solution could be to plan the motion of the object considering that its projection on the ground (including the inertia of the object) does not overlap with the human. In other words, if the robot is transporting a box, it should move the box over human-free space so that in case of an accident the box falls on the floor. Nevertheless, these cases should be further studied.

Multi-robot and multi-human interactions bring new challenges to the human safety problem. The methods proposed in this dissertation should work in a scenario with a single robot and multiple humans, as long as the humans' states are observable and assuming there is enough computational power. Interesting studies found in the literature, such as the one done by Brscic *et al.* where children deliberately sabotage the robot task, indicate that close attention should be paid to intentionally unexpected human behavior [47]. We can foresee a couple of challenges in scenarios with multiple robots and a single human. First, define the appropriate strategy for robots to ensure human safety: a) independently by using safe motions even to other robots but prioritizing the human, or b) collectively as a team where the robots interchange human state information and schedule their motions to minimize the risk of a collision. The methods proposed in this dissertation should be able to follow the strategy (a) but this has to be tested. Regarding the strategy (b), even though the proposed methods do not depend on the source of the human state information (it could be fused from several robots and/or sensors), the generation of coordinated safe motions should be further studied. Second, psychological factors play an important role in the achievement of human safety. As studied by Yang *et al.* [48], Veloso [49], and Sklar *et al.* [50], the Robot-Robot Interaction (RRI) in the presence of humans affects the HRI. For example, if human-unaware communication channels like wireless communication are used, the human may not easily estimate the intentions of the robot group. We can think that a group of robots approaching a human can be frightening which could lead to a human behavior even more erratic than expected. Further research integrating visual and verbal communication channels to decrease this undesired human response and physical human safety such as the one proposed in this dissertation should be pursued.

Future work to standardize reliable methods to evaluate the sense of safety should be done. Even though subjective evaluation inherits the intrinsic bias of the human perception of safety, it is an important tool to determine what methods are accepted as safe by the subjects. At the end, if the users do not trust the robot motions even if they are theoretically (or even experimentally) safe, the adoption of robots in daily-life environments will be slower.

Future work should be done regarding the estimation of the human state

when the sensor information is incomplete or inaccurate. Redundant information provides a clue about the human state but the reliability of this information and its impact on human safety should be further investigated.

The proposed controllers are limited to velocity-independent tasks (e.g., pick-and-place, as opposed to velocity-dependent tasks such as catching a ball). This limitation can be solved with a planner and by studying the interruptibility of the task. Let's consider the case where a robot is juggling some balls. The velocities of the end-effectors are subjected to the task so the strategy of reducing speed is not viable as it will break the task completeness. On the other hand, we can think of a situation where the task is not human-safely feasible but it is possible to bring the robot to a known state where the task can be paused (stop the juggling and catch all the balls) and wait for the safety conditions to be available to restart. This should be further studied.

Further research should be done regarding the evaluation of the proposed safety index in terms of human safety. A common methodology to evaluate human safety is subjective evaluation. A subjective evaluation reflects the human notion of danger at some extent, but it gives a limited (if not null) information about the physical consequences of collisions, e.g., injuries. Another option is to monitor biosignals to evaluate human safety but this is still subject to the human notion of danger. In the absence of a ground truth in the human safety field, a comparison among existing methods is another alternative. Nevertheless, the parametric differences and settings of each method make challenging to achieve a fair comparison. This dissertation used one criteria for the fair comparison but many others should be tested to achieve a comprehensive comparison. For example, another criteria could be that two methods complete the same task but one makes the robot move faster or closer to the human. Moreover, the challenge of evaluating human safety out of controlled or research-oriented environments remains.

Future work on planning for safety should be done as SI can determine which trajectories are safe for the human. SI can traverse a given trajectory and score the danger of every point on the trajectory. If any point on the trajectory violates the safety constraint, then the trajectory is unsafe. Multiple candidate trajectories can be generated to complete the task. A polynomial or a sample-based

algorithm can be used to generate the trajectories. Given the relatively high computational cost of the current implementation of SI, a polynomial is more suitable. Once the trajectories are generated, SI can be used to score the danger for every point. The robot position and velocity are given by the trajectory and the state of the human is observed. For the calculation of the danger score, the human state will be the same. The trajectories that violate the safety constraint are discarded and those candidates that comply can be safely used to complete the task.

Publication list

Refereed Journal Papers

1. **Gustavo Alfonso Garcia Ricardez**, Akihiko Yamaguchi, Jun Takamatsu, and Tsukasa Ogasawara, "Asymmetric Velocity Moderation for Human-Safe Robot Control," *Advanced Robotics*, vol. 29, no. 17, September 2015, pp. 1111–1125.

Refereed International Conference Proceedings Papers

1. **Gustavo Alfonso Garcia Ricardez**, Akihiko Yamaguchi, Jun Takamatsu, and Tsukasa Ogasawara, "Human Safety Index based on Impac Severity and Human Behavior Estimation," *in Proceedings of the 2nd International Conference on Mechatronics and Robotics Engineering (ICMRE)*, Nice, France, February 18-22, 2016.

2. **Gustavo Alfonso Garcia Ricardez**, Akihiko Yamaguchi, Jun Takamatsu, and Tsukasa Ogasawara, "Human Safety and Efficiency of a Robot Controlled by Asymmetric Velocity Moderation," *in Proceedings of the 10th ACM/IEEE International Conference on Human-Robot Interaction Extended Abstracts (HRI 2015)*, Portland, USA, March 2-5, 2015, pp. 183-184.

3. **Gustavo Alfonso Garcia Ricardez**, Akihiko Yamaguchi, Jun Takamatsu, and Tsukasa Ogasawara, "Extended Asymmetric Velocity Moderation: a Reactive Strategy for Human-Safe Robot Control," *in Proceedings of the 2013 IEEE Conference on Robotics and Biomimetics (ROBIO 2013)*, Shenzhen, China, December 12-14, 2013, pp. 450-455.

4. **Gustavo Alfonso Garcia Ricardez**, Akihiko Yamaguchi, Jun Takamatsu, and Tsukasa Ogasawara, "Withdrawal Strategy for Human Safety based on a Virtual Force Model," *in Proceedings of the 2013 IEEE/RSJ International Conference on Intelligent Robots and Systems (IROS 2013)*, Tokyo, Japan, November 3-7, 2013, pp. 1119-1124.

5. **Gustavo Alfonso Garcia Ricardez**, Akihiko Yamaguchi, Jun Takamatsu, and Tsukasa Ogasawara, "Asymmetric Velocity Moderation: a Reactive

Strategy for Human Safety," *in Proceedings of the 10th IEEE International Symposium on Safety, Security, and Rescue Robotics (SSRR 2012)*, College Station, USA, November 5-8, 2012.

Japanese Conference Proceedings Papers

1. **Gustavo Alfonso Garcia Ricardez**, Akihiko Yamaguchi, Jun Takamatsu, and Tsukasa Ogasawara, "Improving the Trajectory Scaling Computation of Asymmetric Velocity Moderation," *in Proceedings of the 32nd Annual Conference of the Robotics Society of Japan (RSJ 2014)*, Fukuoka, Japan, September 4-6, 2014, 2E2-04.

2. **Gustavo Alfonso Garcia Ricardez**, Phawat Lertariyasakchai, Akihiko Yamaguchi, Jun Takamatsu, and Tsukasa Ogasawara, "Kinematic Analysis for the Development of Human-Safe Robot Behavior using a Sensor Suit," *in Proceedings of the 31st Annual Conference of the Robotics Society of Japan (RSJ 2013)*, Tokyo, Japan, September 4-6, 2013, 1J3-01.

3. **Gustavo Alfonso Garcia Ricardez**, Akihiko Yamaguchi, Jun Takamatsu, and Tsukasa Ogasawara, "Efficiency Evaluation of Asymmetric Velocity Moderation based on Task Completion Time," *in Proceedings of the 2013 JSME Conference on Robotics and Mechatronics (ROBOMEC 2013)*, Tsukuba, Japan, May 22-25, 2013, 2A2-I10.

4. **Gustavo Alfonso Garcia Ricardez**, Akihiko Yamaguchi, Jun Takamatsu, and Tsukasa Ogasawara, "Velocity Moderation for Providing Human Safety Reactively," *in Proceedings of the 30th Annual Conference of the Robotics Society of Japan (RSJ 2012)*, Sapporo, Japan, September 17-20, 2012, 4M1-7.

References

[1] B. Gates, "A robot in every home," *Scientific American Magazine*, vol. 296, no. 1, 2007, pp. 58–65.

[2] O. Ogorodnikova, "Methodology of safety for a human robot interaction designing stage," in *Proc. 2008 Human System Interactions Conf.*, May 2008, pp. 452–457.

[3] R. Alami, A. Albu-Schaeffer, A. Bicchi, R. Bischoff, R. Chatila, A. De Luca, A. De Santis, G. Giralt, J. Guiochet, G. Hirzinger, F. Ingrand, V. Lippiello, R. Mattone, D. Powell, S. Sen, B. Siciliano, G. Tonietti, and L. Villani, "Safe and dependable physical Human-Robot Interaction in anthropic domains: State of the art and challenges," in *Workshop Proc. 2006 IEEE/RSJ Int. Conf. on Intelligent Robots and Systems (IROS)*, October 2006, pp. 1–16.

[4] A. De Santis, B. Siciliano, A. De Luca, and A. Bicchi, "An atlas of physical Human-Robot Interaction," *Mechanism and Machine Theory*, vol. 43, no. 3, 2008, pp. 253–270.

[5] Y. Yamada, "Safety robot technology in the future," *Advanced Robotics*, vol. 23, no. 11, 2009, pp. 1513–1516.

[6] T. Fraichard and J. Kuffner, "Guaranteeing motion safety for robots," *Autonomous Robots*, vol. 32, no. 3, 2012, pp. 173–175.

[7] S. Haddadin, *Towards Safe Robots: Approaching Asimov's 1st Law.* Springer Publishing Company, Inc., 2013.

[8] S. Haddadin, A. Albu-Schaffer, A. De Luca, and G. Hirzinger, "Collision detection and reaction: A contribution to safe physical Human-Robot Interaction," in *Proc. 2008 IEEE/RSJ Int. Conf. on Intelligent Robots and Systems (IROS)*, September 2008, pp. 3356–3363.

[9] E. Sisbot, L. Marin-Urias, R. Alami, and T. Simeon, "A human aware mobile robot motion planner," *IEEE Trans. on Robotics*, vol. 23, no. 5, October 2007, pp. 874–883.

[10] E. Sisbot and R. Alami, "A human-aware manipulation planner," *IEEE Trans. on Robotics*, vol. 28, no. 5, October 2012, pp. 1045–1057.

[11] C.-S. Tsai, J.-S. Hu, and M. Tomizuka, "Ensuring safety in human-robot coexistence environment," in *Proc. 2014 IEEE/RSJ Int. Conf. on Intelligent Robots and Systems (IROS)*, September 2014, pp. 4191–4196.

[12] D. Kulić and E. Croft, "Pre-collision safety strategies for Human-Robot Interaction," *Autonomous Robots*, vol. 22, no. 2, 2007, pp. 149–164.

[13] K. Ikuta, H. Ishii, and M. Nokata, "Safety evaluation method of design and control for human-care robots," *International Journal of Robotics Research*, vol. 22, no. 5, 2003, pp. 281–297.

[14] T. Fraichard, "Motion Safety with People: an Open Problem," in *Proc. 2015 IEEE Int. Conf. on Robotics and Automation (ICRA)*, Seattle, United States, May 2015.

[15] ISO-10218, *Robots and robotic devices – Safety requirements for industrial robots, Part 1: Robots*, 2nd ed. ISO, Geneva, Switzerland, 2011.

[16] ISO-13482, *Robots and robotic devices – Safety requirements for personal care robots.* ISO, Geneva, Switzerland, 2013.

[17] ISO/TS-15066, *Robots and robotic devices – Safety requirements for industrial robots – Collaborative operation.* ISO, Geneva, Switzerland, not yet publically available.

[18] D. Kulić and E. A. Croft, "Real-time safety for human–robot interaction," *Robotics and Autonomous Systems*, vol. 54, no. 1, 2006, pp. 1 – 12.

[19] J. Mainprice, E. A. Sisbot, L. Jaillet, J. Cortés, R. Alami, and T. Siméon, "Planning human-aware motions using a sampling-based costmap planner," in *2011 IEEE Int. Conf. on Robotics and Automation (ICRA)*, May 2011, pp. 5012–5017.

[20] H. Ding, G. Reißig, K. Wijaya, D. Bortot, K. Bengler, and O. Stursberg, "Human arm motion modeling and long-term prediction for safe and

efficient human-robot-interaction," in *Proc. 2011 IEEE Int. Conf. on Robotics and Automation (ICRA)*, 2011, pp. 5875–5880.

[21] J. Heinzmann and A. Zelinsky, "Quantitative safety guarantees for physical human-robot interaction," *The International Journal of Robotics Research*, vol. 22, no. 7-8, 2003, pp. 479–504.

[22] S. Parusel, S. Haddadin, and A. Albu-Schaeffer, "Modular state-based behavior control for safe human-robot interaction: A lightweight control architecture for a lightweight robot," in *Proc. 2011 IEEE Int. Conf. on Robotics and Automation (ICRA)*, May 2011, pp. 4298–4305.

[23] J.-J. Park, S. Haddadin, J.-B. Song, and A. Albu-Schäffer, "Designing optimally safe robot surface properties for minimizing the stress characteristics of human-robot collisions," in *2011 IEEE Int. Conf. on Robotics and Automation (ICRA)*, 2011, pp. 5413–5420.

[24] O. Ogorodnikova, "How safe the human-robot coexistence is? Theoretical presentation," *Acta Polytechnica Hungarica*, vol. 6, no. 4, 2009, pp. 51–74.

[25] S. Kotosaka and R. Hodoshima, "Risk estimation for human-symbiotic-robot based on the analysis of human motion," in *Proc. 30th Annual Conf. of the Robotics Society of Japan (RSJ)*, Sapporo, Japan, September 2012, pp. 4M2–6.

[26] B. Lacevic and P. Rocco, "Kinetostatic danger field - a novel safety assessment for Human-Robot Interaction," in *Proc. 2010 IEEE/RSJ Int. Conf. on Intelligent Robots and Systems (IROS)*, 2010, pp. 2169–2174.

[27] B. Lacevic and P. Rocco, "Safety-oriented path planning for articulated robots," *Robotica*, vol. 31, September 2013, pp. 861–874.

[28] S. Haddadin, A. Albu-Schaffer, M. Frommberger, J. Rossmann, and G. Hirzinger, "The 'DLR Crash Report': Towards a standard crash-testing protocol for robot safety - Part I: Results," in *Proc. 2009 IEEE Int. Conf. on Robotics and Automation (ICRA)*, May 2009, pp. 272–279.

[29] S. Haddadin, A. Albu-Schaffer, M. Frommberger, J. Rossmann, and G. Hirzinger, "The 'DLR Crash Report': Towards a standard crash-testing protocol for robot safety - Part II: Discussions," in *Proc. 2009 IEEE Int. Conf. on Robotics and Automation (ICRA)*, May 2009, pp. 280–287.

[30] T. Ogure, Y. Nakabo, S. Jeong, and Y. Yamada, "Hazard analysis of an industrial upper - body humanoid," *Industrial Robot: An International Journal*, vol. 36, no. 5, 2009, pp. 469–476.

[31] S. Haddadin, S. Haddadin, A. Khoury, T. Rokahr, S. Parusel, R. Burgkart, A. Bicchi, and A. Albu-Schäffer, "On making robots understand safety: Embedding injury knowledge into control," *The International Journal of Robotics Research*, vol. 31, no. 13, 2012, pp. 1578–1602.

[32] J. Echávarri, M. Ceccarelli, G. Carbone, C. Alén, J. L. Muñoz, A. Díaz, and J. M. Munoz-Guijosa, "Towards a safety index for assessing head injury potential in service robotics," *Advanced Robotics*, vol. 27, no. 11, 2013, pp. 831–844.

[33] E. Szádeczky-Kardoss and B. Kiss, "Tracking error based on-line trajectory time scaling," in *Proc. 2006 Int. Conf. on Intelligent Engineering Systems (INES)*, 2006, pp. 80–85.

[34] D. Helbing and P. Molnár, "Social force model for pedestrian dynamics," *Physical Review E*, vol. 51, May 1995, pp. 4282–4286.

[35] M. Luber, J. Stork, G. Tipaldi, and K. Arras, "People tracking with human motion predictions from social forces," in *Proc. 2010 IEEE Int. Conf. on Robotics and Automation (ICRA)*, May 2010, pp. 464–469.

[36] T. I. Lakoba, D. J. Kaup, and N. M. Finkelstein, "Modifications of the Helbing-Molnár-Farkas-Vicsek social force model for pedestrian evolution," *Simulation*, vol. 81, no. 5, May 2005, pp. 339–352.

[37] P. Ratsamee, Y. Mae, K. Ohara, T. Takubo, and T. Arai, "Modified social force model with face pose for human collision avoidance," in *Proc. 7th Annual ACM/IEEE Int. Conf. on Human-Robot Interaction (HRI)*, March 2012, pp. 215–216.

[38] K. Kaneko, F. Kanehiro, M. Morisawa, K. Akachi, G. Miyamori, A. Hayashi, and N. Kanehira, "Humanoid robot HRP-4 – humanoid robotics platform with lightweight and slim body," in *Proc. 2011 IEEE/RSJ Int. Conf. on Intelligent Robots and Systems (IROS)*, 2011, pp. 4400–4407.

[39] I. Chen, B. MacDonald, B. Wünsche, G. Biggs, and T. Kotoku, "A simulation environment for openrtm-aist," in *Proc. IEEE Int. Symposium on System Integration*, vol. 29, 2009, pp. 113–117.

[40] R. Diankov, "Automated construction of robotic manipulation programs," Ph.D. dissertation, Carnegie Mellon University, Robotics Institute, August 2010.

[41] P. K. Agarwal, H. Edelsbrunner, O. Schwarzkopf, and E. Welzl, "Euclidean minimum spanning trees and bichromatic closest pairs," *Discrete & Computational Geometry*, vol. 6, no. 1, 1991, pp. 407–422.

[42] J. L. Bentley, "Multidimensional binary search trees used for associative searching," *Commun. ACM*, vol. 18, no. 9, Sep. 1975, pp. 509–517.

[43] T. Cover and P. Hart, "Nearest neighbor pattern classification," *IEEE Transactions on Information Theory*, vol. 13, no. 1, January 1967, pp. 21–27.

[44] S. Haddadin, A. Albu-Schäffer, and G. Hirzinger, "Safe physical Human-Robot Interaction: Measurements, analysis and new insights," in *Proc. 13th Int. Symp. on Robotics Research (ISRR)*, November 2007, pp. 395–407.

[45] T. Malm, J. Viitaniemi, J. Latokartano, S. Lind, O. Venho-Ahonen, and J. Schabel, "Safety of interactive robotics – learning from accidents," *International Journal of Social Robotics*, vol. 2, no. 3, 2010, pp. 221–227.

[46] M. D. Zeiler, "ADADELTA: an adaptive learning rate method," *CoRR*, vol. abs/1212.5701, 2012.

[47] D. Brscić, H. Kidokoro, Y. Suehiro, and T. Kanda, "Escaping from children's abuse of social robots," in *Proc. 10th Annual ACM/IEEE Int. Conf. on Human-Robot Interaction*, New York, NY, USA, 2015, pp. 59–66.

[48] J.-Y. Yang and D.-S. Kwon, "The effect of multiple robot interaction on human-robot interaction," in *Proc. 9th Int. Conf. on Ubiquitous Robots and Ambient Intelligence (URAI)*, Nov 2012, pp. 30–33.

[49] M. Veloso, "A few issues on human-robot interaction for multiple persistent service mobile robots," in *Proc. AAAI Fall Symposium Series*, 2014.

[50] E. Sklar, E. Schneider, A. T. Ozgelen, and M. Azhar, "Toward human/multi-robot systems to support emergency services agencies," in *Proc. AAAI Fall Symposium Series*, 2014.